UNIVERSITY OF TARTU
Faculty of Science and Technology
Institute of Physics

Shania Roy

Investigation of luminescence properties of wide gap BaY_2F_8 and KY_3F_{10} single crystals by means of luminescence spectroscopy

Master's Thesis (30 ECTS)

Supervisor:

Prof. Marco Kirm
Laboratory of Ionic crystal
Institute of Physics
University of Tartu

Tartu 2021

Investigation of luminescence properties of wide gap BaY_2F_8 and KY_3F_{10} single crystals by means of luminescence spectroscopy.

Abstract:

The present study was devoted to the investigation and identification of various kinds of intrinsic emissions in BaY_2F_8 and KY_3F_{10} single crystals. Both compounds belong to the materials with cross-luminescence, which is due to the recombination of electrons from the valence F 2p states with Ba 5p or K 3p core holes, respectively. The extensive spectroscopic studies were performed using cathodoluminescence and time resolved luminescence spectroscopy under synchrotron radiation at various temperatures. The obtained experimental results were used to identify electronic band structure parameters such as the exciton formation energy E_{exc}, the energy gap value E_g and the ionization energy of cation levels E_{gc}. These values were compared with those obtained in theoretical studies of electronic band structures available in public databases of materials properties (AFLOW, Materials Project).

It was found that in BaY_2F_8 cross-luminescence covers the energy range from 7.6 to 5.0 eV, with its excitation onset is at 19.3 eV. The energy gap value estimated $E_g \sim 11.4$ eV, thus, the Ba 5p are separated from the top of the valence band by 7.9 eV. Low temperature luminescence bands in the UV – visible range are shown to be non-elementary, consisting of the STE emission peaked at 4.96 eV (E_{exc}=10.35 eV) and some defect or impurity emission peaking at 3.8 eV. Decay kinetics analysis performed for ultrafast UV emissions show that they contain three exponential components with sub- and nanosecond lifetimes typical for cross-luminescence.

In KY_3F_{10} single crystal, cross-luminescence was revealed in the energy range from 9.1 to 6.0 eV. The excitation peak for 4.5 eV emission observed at 9.9 eV near the intrinsic absorption edge is assigned to the creation of excitons and the energy gap value is estimated to $E_g \sim 11.4$ eV. The analysis of time integrated excitation spectra for UV emissions revealed several features in the energy range of 28.7 – 32.5 eV, which according to the theoretical results are due to the contribution of the Y 4p states. The Y 4p states are energetically located below the K 3p levels that prohibits their participation in the relaxation processes of excitations related to the higher lying K 3p core and valence band. The UV emissions near 5.0 eV are tentatively assigned to defect and impurity centers, while a broad emission band with maximum at 3.6 eV is attributed to STE. In the decay kinetics of the UV luminescence in KY_3F_{10}, three exponential components with sub- and nanosecond lifetimes were identified.

This research shows how important is to combine contemporary time-resolved spectroscopic investigations at modern light sources and the results of advanced electronics structure calculations in order to understand luminescence properties of wide gap scintillators. Such analysis greatly promotes a progress in scintillator science and technology of optical materials urgently needed in many applications.

Keywords: wide gap crystals, intrinsic emissions, cross-luminescence, self-trapped excitons, ternary fluorides, time resolved luminescence spectroscopy, luminescence decay kinetics, synchrotron radiation.

CERCS: P260 Condensed matter: electronic structure, electrical, magnetic and optical properties, supraconductors, magnetic resonance, relaxation, spectroscopy; T151 Optical materials.

Laia keelutsooniga BaY_2F_8 ja KY_3F_{10} monokristallide omaduste luminestsentsspektroskoopilised uuringud

Lühikokkuvõte:

Käesolev töö on pühendatud erinevate omakiirguste uurimisele ja identifitseerimisele BaY_2F_8 ja KY_3F_{10} monokristallides. Mõlemad ühendid kuuluvad materjalide hulka, milles on leitud kross-luminestsents, mis tekib F 2p valentselektronide rekombinatsioonil, vastavalt kas Ba 5p või K 3p katiooni aukseisunditega. Töö käigus viidi läbi mahukad spektraaluuringud kasutades katoodluminestsentsi ja ajalise lahutusega luminestsentsspektroskoopiat ergastamisel sünkrotron-kiirgusega erinevatel temperatuuridel. Saadud eksperimentaalsetest andmetest määrati sellised ainete elektronstruktuuri parameetrid nagu eksitonide tekitamise energia E_{exc}, keelutsooni laius E_g ja katioonseisundite ionisatsiooni energia E_{gc}. Saadud väärtusi võrreldi teoreetiliste arvutuste tulemustega, mis on kättesaadavad avalikes andmebaasides nagu AFLOW ja Materials Project.

BaY_2F_8 puhul leiti, et kross-luminestsents katab energia piirkonna 7.6 – 5.0 eV ning selle ergastuslävi asub 19.3 eV. Keelutsooni laiuseks hinnati $E_g \sim 11.4$ eV. Seega, Ba 5p seisundid asuvad valentsitsooni laest 7.9 eV kaugusel. Madalatemperatuursed kiirgusribad UV ja nähtavas spektraalpiirkonnas on mitte-elementaarsed ja koosnevad iselõksustunud eksitoni kiirgusest energiaga 4.96 eV (E_{exc}=10.35 eV) ning defekti-lisandi kiirgusest 3.8 eV. Ülikiire UV kiirguse kustumiskineetika analüüs näitas, et seda saab lähendada kolme eksponentfunktsiooniga sub-ns ja nanosekundilises piirkonnas, on tüüpilised kross-luminestsentsi eluead.

KY_3F_{10} kristalli jaoks leiti, et kross-luminestsents katab energia piirkonna 9.1 – 6.0 eV. Fundamentaalneeldumise serval leitud ergastusriba 9.9 eV, 4.5 eV kiirguse jaoks, on seotud eksitonide tekkega ning keelutsooni väärtuseks hinnati $E_g \sim 11.4$ eV. Ajaliselt integreeritud UV kiirguse ergastusspektritest leiti, et struktuurid 28.7 – 32.5 eV piirkonnas on seotud Y 4p ergastustega vastavalt tsoonistruktuuri arvutustele. Seega Y 4p seisundid asuvad sügavamal kui K 3p seisundid ja seepärast ei võta osa ei kross-luminestsentsiga ega ka teisestest valentsergastustega seotud relaksatsiooni protsessidest. UV kiirgused 5.0 eV ümbruses on esialgselt tõlgendatud defekti-lisandi tsentrite kiirgusena ning laiaribalise iselõksustunud eksitoni kiirguse asukohaks spektris on riba 3.6 eV juures. KY_3F_{10} UV kiirguse kustumiskineetikas leiti kolm eksponentsiaalset komponenti eluigadega sub-ns ja nanosekundilises piirkonnas.

Selle magistritöö raames tehtud uuringud näitavad ilma kahtluseta kui oluline on kasutada kaasaaegseid ajalise lahutusega spektroskoopilisi uuringuid koos modernsete valgusallikatega ning kaugele arendatud tsoonistruktuuri teoreetiliste arvutuste tulemusi, et aru saada laia keelutsooniga stsintillaatorite luminestsentsomadustest. Sellised materjalide omaduste analüüsid aiatavad kaasa progressile stsintillaatorite uuringutes ning optiliste materjalide tehnoloogias, mida vajatakse paljudes rakendustes.

Võtmesõnad: laia keelutsooniga kristallid, omakiirgused, kross-luminestsents, iselõksustunud eksiton, ternaarsed fluoriidid, aeg-lahutusega luminestsentsspektrsokoopia, luminestsentsi kustumise kineetika, sünkrotron kiirgus.

CERCS: P260 Tahke aine: elektrooniline struktuur, elektrilised, magneetilised ja optilised omadused, ülijuhtivus, magnetresonants, spektroskoopia; T151 Optilised materjalid.

Contents

ABBREVIATIONS

AFLOW	Automatic - Flow for Material Discovery
CL	Cross-luminescence
CCD	Charge-coupled device
CLU	Cathodoluminescence
E_g	Energy gap
E_{exc}	Exciton formation energy
E_{gc}	Cation energy gap
E_{cv}	Energy gap between outermost core band and valence band
FWHM	Full Width at Half Maximum
IRF	Instrumental Response Function
IF	Intermediate Frequency
MCP-PMT	Micro Channel plate- Photomultiplier tube
PMT	Photomultiplier tube
PL	Photoluminescence
RT	Room temperature
STE	Self-trapped Exciton
SR	Synchrotron Radiation
TW	Time Window
TI	Time Integrated
UV	Ultraviolet
VUV	Vacuum Ultraviolet
XUV	Extreme ultraviolet

1. Introduction

In the early days, people were creating light from chemical means, but nowadays modern society deliberately depends on mankind's ability to produce light in more advanced ways. With more technological approaches, it is important to understand the underlying physical and chemical processes, which results in the luminescence of solids. For example, along with researching light generation processes many other useful phenomena can be found and be exploited in various technology [1].

All solids are absorbing electromagnetic radiation, which undergoes complicated relaxation processes and under favorable conditions, it may result in luminescence, where generally emitted photons have lower energy than the absorbed radiation due to the longer wavelength. There are different kinds of luminescence centers are available. These centers can be classified as intrinsic and extrinsic emissions. Intrinsic emissions are introduced due to the electronic excitations created in the host material, whereas extrinsic emissions are caused by the impurity or defect centers, which are either doped intentionally or introduced during the sample preparation. Thus, in order to exploit luminescence materials, one should be able to separate different kinds of emissions, understand their excitation mechanisms, which allows their knowledge-based use in various applications. This master's thesis is devoted to the investigation of relaxation processes of electronic excitations and luminescence properties of barium yttrium fluoride (BaY_2F_8) and potassium yttrium fluoride (KY_3F_{10}) single crystals. The main goal is to understand the role and properties of different relaxation channels: cross-luminescence (which is discussed below), other kinds of intrinsic and extrinsic emissions such as self-trapped exciton (STE) emission, and dopant ions. Quite often different kinds of emissions are overlapping but can be distinguished on the basis of their decay times, which can be recorded for each wavelength. This is also the focus of the master thesis- how to separate emission originating from different centers by spectrally and time-resolved spectroscopy.

None of the materials are perfect because extrinsic emission centers, introduced due to either a chemical impurity or an imperfection in the regular spacing of the atoms that invent the crystal structure. While studying crystalline materials where Y is in the composition, we mostly expect the introduction of other rare-earth ions, which inseparably contaminate host material with Yttrium in ppm-level. Usually, electronic states of impurity ions are located within the energy gap and can be excited directly through intra-center excitation or by energy transfer processes

from the host. Despite the forbidden nature of 4f-4f emissions of rare-earth ions, their narrow line luminescence is well separable from broadband intrinsic emissions. Impurity luminescence is rather a temperature stable and can be observed from liquid helium to room temperature. At higher temperatures, non-radiative decay may occur. It is important to note that temperature behavior and the particular quenching temperatures are host and impurity center-specific.

Intrinsic emissions stem from the electronic structure of the host lattice. The intrinsic emissions are efficiently excited in the fundamental absorption region. It starts with a formation of exciton states composed of a bound electron-hole pair (a zero-net charge) and at higher energies, a free electron is lifted to the conduction band and a hole in the valence band is created. The lowest energy of this corresponds to the energy gap value E_g and is an important parameter of the band structure of the material. The relaxation of electron-hole pairs and excitons results in self-trapped exciton formation because of this energetically most favorable relaxed state [2]. Self-trapped exciton (STE) may decay radiatively or transfer to other extrinsic emission centers. There is a restriction of the movement of charged electrons and holes in any location of a solid (mostly in an insulator and a semiconductor) within a crystal structure, but they can be trapped at various centers and finally may recombine with their counterparts resulting in luminescence. self-trapped excitons have two typical features: a large Stokes shift and a broadband emission spectrum with the FWHM (full width at half maximum), which is usually larger than 100 nm. Usually, STE's are stable at low temperatures, but at higher temperatures (typically below room temperature) their thermal destruction occurs. The self-trapped exciton is typically formed in the recombination of an electron with a stable self-trapped hole [2], resulting in its radiative decay and annihilation of STE. Self-trapped exciton luminescence, radiative recombination with electron and holes [3]. (without exciton formation) and cross-luminescence belong to various types of intrinsic emissions. Cross-luminescence is introduced due to the radiative recombination of electrons from the anion valence bands with the holes in the uppermost cation core band. The latter emission can be observed in wide-gap materials with specific properties (see the literature overview section).

The present research of my Master's Thesis is important in distinguishing different relaxation processes of electronic excitations in wide-gap materials, learn about their luminescence properties using advanced time-and-spectrally resolved luminescence spectroscopy. It will contribute to the design of novel light-emitting materials, including scintillators with ultrafast emissions.

2. Literature Overview

The origin of cross luminescence was proven in the early 1980s, and it was observed only in the six binary ionic crystals, specifically in KF, BaF_2, CsF, CsCl, CsBr, and RbF. It was also revealed in several multi-component and ternary crystals, which are based on these six above-mentioned binary compounds. Since its discovery, this novel phenomenon was considered as appropriate for the scintillation applications as well [4].

The cross-luminescence takes place in materials, where there an energetic separation of outermost core level to valence band is smaller than an energy gap of the material. CL is only observable in materials in which the Auger decay is prohibited since the energy gap E_{CV} between the top of the outermost core band and the top of the valence band is smaller than the energy gap E_g between the valence and the conduction band ($E_{CV} < E_g$). It has been shown that cross-luminescence has no temperature quenching until the temperature range up to 700K. It is not affected by the temperature, because the valence band to the core level separation is significant (several eV) in comparison with the phonon energies in the meV range. It means that in wide energy gap crystals [5] there are no other processes (energy transport), which could influence the decay time of cross-luminescence being solely determined by the very short lifetime of the core hole. For the same reasons, cross-luminescence has no rise time, which is important for high time-resolution scintillation applications.

Thus, the cross-luminescence can only be excited by the photons or the particles along with the sufficient energy which can create holes in the uppermost cation core band and hence, corresponding to the cation's ionization energies have a threshold in the optical excitation spectra. One of such examples is shown in Fig.1 where the cross-luminescence mechanism along with radiative relaxation of other electronic excitations is depicted for barium fluoride (BaF_2) [6].

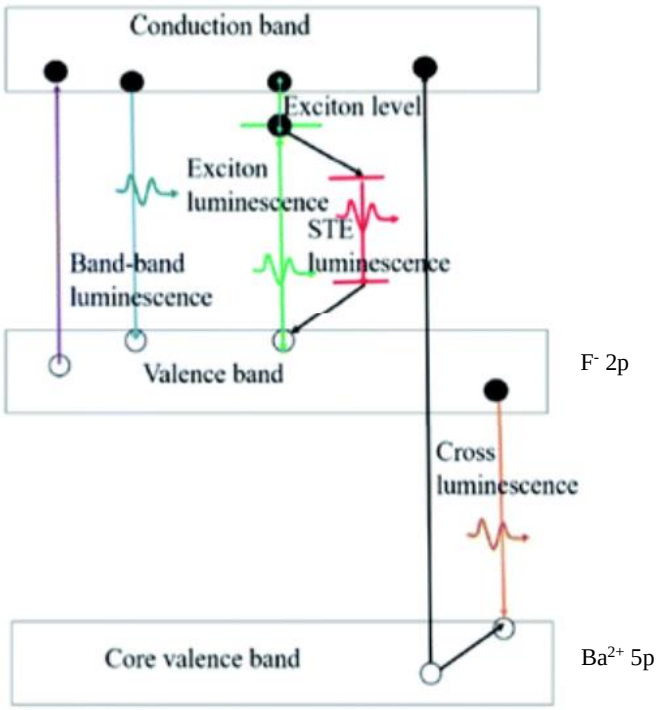

Fig. 1. A schematic of various intrinsic luminescence phenomena, including band-to-band luminescence, exciton luminescence, STE luminescence, and cross luminescence [6].

In Fig. 1, shows the general schematic diagram of the various intrinsic luminescence phenomena in wide gap materials. The cross-luminescence will occur when an electron in the valence band and a hole in the outermost core band is recombined (as discussed above). Exciton luminescence comprises that the bound state of an electron and a hole, which attracts each other by the electrostatic Coulomb force and after their recombination, can emit a photon. Furthermore, a relaxed exciton can also be observed, which is called self-trapped exciton (STE), which has typically broad band emission at much lower energies than the energy gap of the host materials. Due to a large Stokes shift STE luminescence do not suffer self-absorption, which is leading to losses in hosts with impurity emissions with a Stokes shift [7].

In Fig. 1, the cross-luminescence and the self-trapped exciton luminescence are shown by arrows in barium fluoride. As the energy gap value E_g=11.23 eV [8] is significantly larger than the energy difference of energy bands (~6.6 eV) between the 2p (F^-) valence band and the 5p (Ba^{2+}) outermost core band. Cross-luminescence is observed in the wavelength range from 170-300 nm and it is spectrally overlapping with the self-trapped exciton emission (both shown in Fig. 1) peaked at 280 nm [9].

There has been considerable interest to other Ba compounds like BaY_2F_8 monoclinic crystals because of their great potential in scintillation applications [10]. BaY_2F_8 crystals have a wide transparency range extending to vacuum ultraviolet (VUV) and their crystal lattice has low symmetry and phonon energies are rather low.

Complex halide crystals are also known as materials with cross-luminescence. Early studies under pulsed electron beam excitation have shown that potassium-containing materials like K_2LiGaF_6, K_2SiF_6, K_2YF_5, and KYF_4 possess cross-luminescence [11]. Cubic KY_3F_{10} has been less investigated and there is not so much known about intrinsic emissions under excitation in the fundamental absorption range.

2.1 Electronic band structure and luminescence properties of barium fluoride (BaF_2) & barium yttrium fluoride (BaY_2F_8)

Early studies showed that the spectral properties of the BaY_2F_8 are rather similar to the BaF_2 crystal. According to this publication, the monoclinic BaY_2F_8 crystal has an energy gap value of 12.4 eV, and the first reflection peak at around 11.7 eV is assigned to the formation of anion excitons [12]. Analogously to BaF_2 the BaY_2F_8 possess self-trapped exciton emission peaked at 4.6 eV (270 nm), which is dominating emission at low temperatures. The self-trapped exciton emission in BaY_2F_8 is quenched above 200 K, which is better for fast scintillation applications at 300 K because only CL is observed in comparison to BaF_2 with still strong STE emission at RT. In BaY_2F_8 the onset of cross-luminescence excitation is found at 19.3 eV and thus the condition $E_{CV} < E_g$ is fulfilled. The earlier studies have shown that fast cross-luminescence covers energy range 3-7 eV under VUV excitation [10], whereas more recent studies under XUV excitation show that CL extends to 7.5 eV [13].

The cross-luminescence decay time in BaY_2F_8 can be fitted with two exponentials τ_1 =0.64 and τ_1 =1.35 ns, being a bit slower than in BaF_2 [14]. By the introduction of the BaF_2 the rare earth elements with the unfilled 4f-orbital, the longer luminescence of the STE is suppressed, also the intensity of fast cross-luminescence is diminishing as well [15].

The electronic band structure of the BaF_2 crystals is the most significant characteristic describing the occupied and unoccupied state of the cations and anions forming the binary compound. The increasing availability of such calculations contributes to the interpretation of relaxation processes of electronic excitations and experimentally observed luminescence bands. Fig. 2 shows the electronic band structure of the BaF_2 crystals and it is provided by the AFLOW (Automatic - Flow for Material Discovery) repository [23]. Valence band due to F 2p states has a width of 1.4 eV. The bottom of the conduction band is due to Ba 5d and 6s states and the fitted band gap value is 9.83 eV, which is 1.4 eV less than experimentally determined E_g=11.23 eV [8]. It is known to be that the density functional theory tends to underestimate energy positions of excited states [17]. The Ba 5p cation states are 8 eV below the top of the valence band.

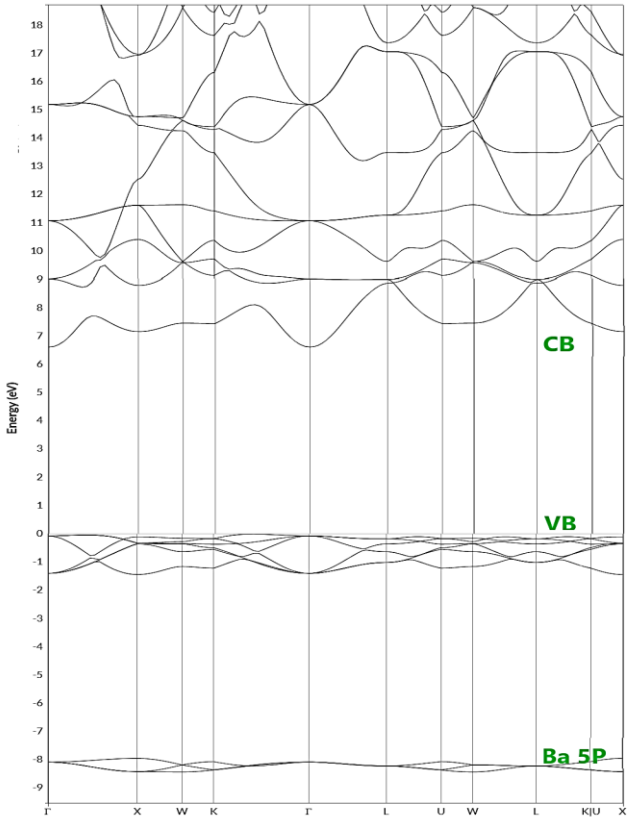

Fig. 2. Calculated electronic band structure of the barium fluoride (BaF_2) from the AFLOW database.

Thus, the energetic distance between the bottom of the F^- 2p valence band and the top of the Ba^{2+} 5p outer-most core band is about 6.6 eV, and its width is 0.5 eV. The high energy edge of CL spectra is at 7.4 eV as shown by experiments under XUV excitation [18], which is in quite good correspondence with the band structure calculations shown in Fig. 2. On the other hand, the low energy edge at 4 eV does not fit so well. The states involved in cross-luminescence have been calculated in the molecular cluster approach [19], resulting in the spectrum with ca 2 eV width, which is less than the value 3.4 eV of experimentally observed. Fig. 3 shows the cubic fluorite crystal structure of BaF_2.

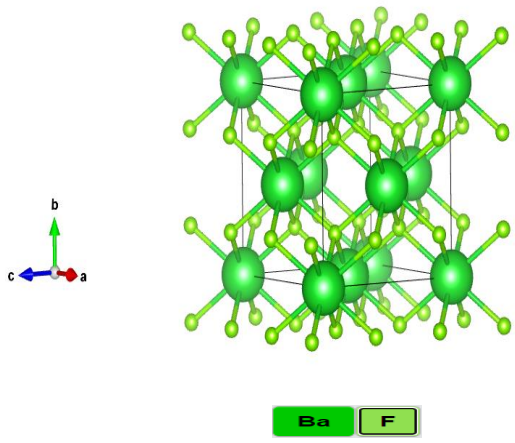

Fig. 3. Crystal structure of the barium fluoride (BaF_2) compound. Dark green spheres are for Ba & the light green spheres are for F ion.

Fig. 3 depicts the 3D structure of the BaF_2 compound, which crystallizes in the cubic Fm-3m space group. Ba^{2+} ions are bonded in a body-centered cubic geometry to eight equivalent F1-atoms [20]. All Ba-F bond lengths are 2.72 Å. F1-is bonded to four equivalent Ba^{2+} atoms to form a mixture of edge and corner-sharing F-Ba_4 tetrahedra.

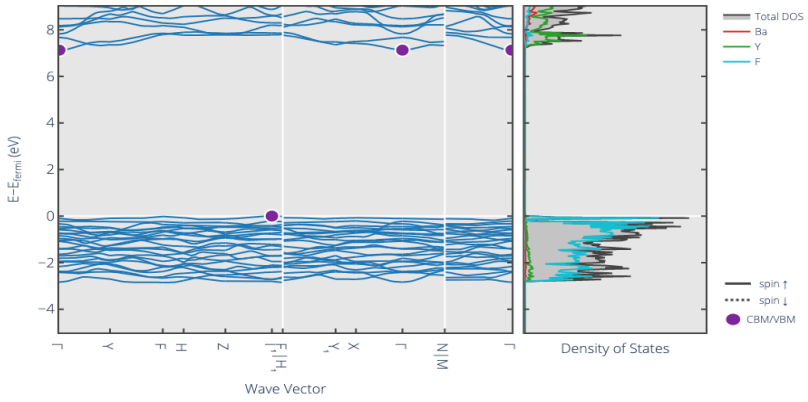

Fig. 4. Calculated electronic band structure of the barium yttrium fluoride (BaY_2F_8) crystal from Materials Project database [20].

Although the number of calculated electronic band structures for all states is increasing, it is not available for all compounds. The calculated electronic band structure of the BaY_2F_8 shown in Fig. 4 was found in the Materials Project database [22], which provides open web-based access to compute information on known materials and predicted ones. Only the valence and conduction band states were available for BaY_2F_8 and therefore there is no information on the Ba 5p cation states, which are directly involved in cross-luminescence transitions. The valence bandwidth is ~2.4 eV being about 1 eV wider than in BaF_2. The bottom of the conduction band is formed from Ba 5d and 6s states analogously to BaF_2. Thus, one can expect an even broader spectrum of cross-luminescence due to the wider valence bandwidth than in BaF_2. The Y^{3+} ion has its outermost 4p band even deeper below the Ba 5p band. According to an early study, as shown by Yu M. Aleksandrov *et al*. [12], the regions where Ba 5p and Y 4p excitation occur are above 18 and 30 eV, respectively. The band structure calculation available in the AFLOW database indicates that the spin-orbit split Y 4p states are located ~17.5 and ~19.5 eV below the top of the valence band in YF_3 (ICSD#26595). By adding a fitted energy gap value of 11.12 eV of YF_3, the respective electronic transitions are expected to occur above 29 eV in agreement with earlier studies. Thus, in BaY_2F_8, in the energy scale, the Y 4p states are below the Ba 5p states and do not contribute to the formation of the cross-luminescence spectrum.

Early studies of pure BaY_2F_8 have established that the first intensive reflection peak occurs at 11.7 eV, which has been assigned to the creation of anion excitons, as reveal by Yu M. Aleksandrov *et al*. [12]. Based on analogy with BaF_2 the value of the energy gap has been

estimated to be equal to E_g=12.4 eV in the same work. A study of Er-, Pr, doped, and undoped BaY_2F_8 single crystals give a smaller value E_g=11.2 eV estimated from the excitation spectra of STE emission [21].

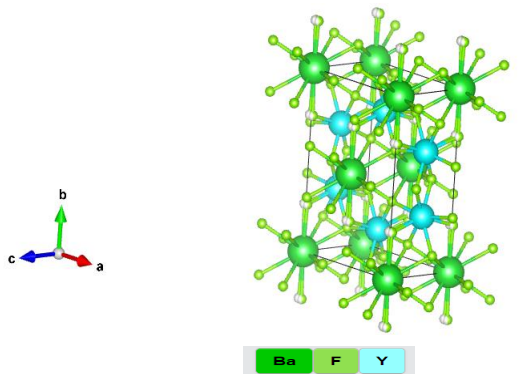

Fig. 5. Crystal Structure of the (BaY_2F_8) crystal. Dark green spheres are for Ba ion, light green spheres are for F ion & sky-blue spheres are for Y ion.

Fig. 5 depicts the 3D structure of the BaY_2F_8 compound, which crystallizes into the monoclinic structure belonging to the C2/m space group. To form face-sharing BaF_{12} cuboctahedra, Ba^{2+} ions are bonded to twelve F1- atoms. There is a layout of Ba-F bond distances ranging from 2.76-2.99 Å. Y^{3+} is bonded in an 8-coordinate geometry to eight F1- atoms. Also, there is a spread of the Y-F bond distance ranging from 2.27-2.35 Å [22].

Table 1. Crystal Structure parameters of the BaF_2 (AFLOW) [23] and BaY_2F_8 compounds (Materials Project) [22].

Specifications	**BaF_2**	**BaY_2F_8**
Crystal Class	Hexoctahedral	Monoclinic

Space Group & Lattice parameter	Fm-3m (# 225)
	a, b, c = 6.28 Å;
		C2/m
		a= b= 6.393Å;
		c= 4.334 Å;

Lattice System	Cubic	Cubic
Lattice Variation	FCC	FCC
Mass Density	4.71 g/cm^3	4.81 g/cm^3
Attenuation Length	2.38 cm	-
Electronic and Fitted bandgap	6.62 eV and 9.83 eV	7.273 eV
Bandgap type	Insulator indirect	Insulator indirect gap I-Γ

2.2 Electronic band structure and luminescence properties of potassium yttrium fluoride (KY_3F_{10})

Potassium yttrium fluoride single crystal has an excellent attractive thermo-mechanical property, possesses wide transparency at the VUV to the infrared region and a great number of potential emitting levels, and has a high optical damage threshold [24]. Therefore, it has been extensively studied as a laser host crystal. It can be activated by different rare-earth ions, which can easily be substituted for single Y^{3+} ions in a non-center symmetrical site without a need for charge compensation. Its crystalline structure provides very low phonon energies (approximately 500 cm^{-1}) avoiding the energy loss by the non-radiative relaxation processes in the KY_3F_{10} crystals [25].

Much less is known about the properties of host electronic excitations in the fundamental absorption range, which is situated in the vacuum ultraviolet (VUV) range analogously to other binary and ternary fluorides. According to the band structure calculation from the AFLOW database [26], KY_3F_{10} has an energy gap value of 6.94 eV, and the corrected "fitted band gap value" is 10.27 eV. Fig.6 displays the band structure calculations of the potassium yttrium fluoride compound. KY_3F_{10} is the cubic crystals with rather a broad valence band with a width of 3.1 eV, mainly originating from F^- 2p states. The energetic distance between the top of the

F^- 2p valence band and narrow K 3p outermost core band is about 9.3 eV, which facilitates the observation of cross-luminescence transitions (9.3 eV < 10.27 eV). Y 4p states form a relatively broadband ~1.5 eV located 17.33 eV below the top of the valence band. Thus, these transitions do not modify cross-luminescence spectra due to recombination of the K 3p holes with F^- 2p.

Although there are no reports on the investigation of optical properties for KY_3F_{10} in VUV, some comparison can be performed with the other analogous KF-based fluorides reported in the literature [27]. According to Makhov and Khaidukov, the cross-luminescence excitation threshold for KYF_4 and $KLuF_4$ crystals is at 20.8 eV, whereas in ternary $KMgF_3$ it is at a higher energy at 21.8 eV as revealed by Kamenskikh et al.[14]. The decay times of cross-luminescence are 1.1 ns in KYF_4 and in $KMgF_3$ two components have been identified τ_1=0.8 and τ_2=1.83 ns, respectively [14]. The cross-luminescence spectra in KYF_4 extend from 5 to 9 eV [30] and similar behavior can be expected for KY_3F_{10}. Fig. 7 shows cross-luminescence spectra of various multi-elemental KF-based wide gap materials under soft X-ray excitation (1 keV photons) at RT [10]. Since electronic states due to Li, Ga, Lu atoms are below the K 3p states, the classical F → K recombination is observed with cross-luminescence in the UV-VUV range.

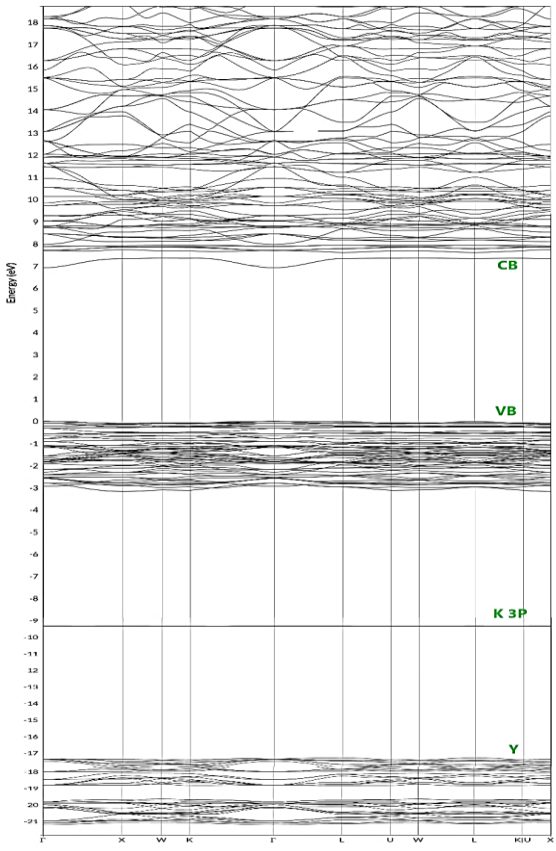

Fig. 6. Band Structure calculation of the potassium yttrium fluoride (KY_3F_{10}) from AFLOW database [30].

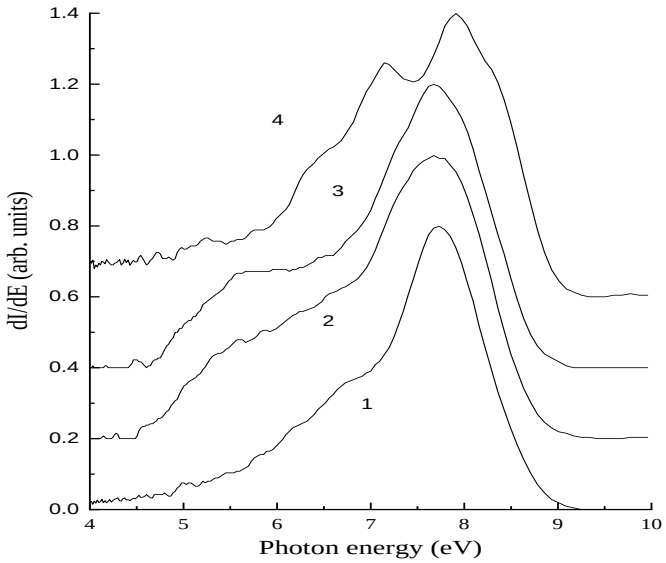

Fig. 7. Cross-luminescence spectra of KYF_4 (1), $KLiYF_4$ (2), $KLiLuF_4$ (3) and $KLiGaF_6$ (4) measured as fast components of emission spectra excited by soft x-ray (~1 keV) SR pulses at S-60 synchrotron [28].

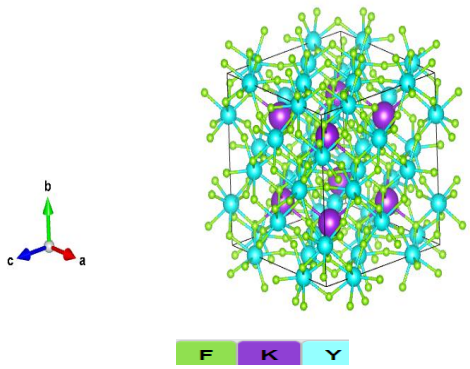

Fig. 8. Crystal structure visualization of the potassium yttrium fluoride (KY_3F_{10}). Purple spheres are for K ion, green spheres are for F ion and sky-blue spheres are for Y ion.

Fig.8, shows the 3D crystal structure of the KY_3F_{10} compound, which belongs to the trigonal R3m space group. K^+ is 7-fold coordinated to seven F^- atoms. There are two different bond lengths, one shorter (2.75 Å) and six longer (3.00 Å), for the K-F bond. To form a distorted

corner-sharing, Y^{3+} bonded to seven F^{-} atoms. There is a layout of Y-F bond distance ranging from 2.17-2.67 Å [29].

Table 2. Crystal Structure parameter of the KY_3F_{10} material (AFLOW) [30].

Specifications	**KY_3F_{10}**
Crystal Class	hexoctahedral
Space Group &Lattice parameter	R3m a,b,c = 11.71Å;
Lattice System	Cubic
Lattice Variation	FCC
Mass Density	4.11 g/cm^3
Attenuation Length	2.97 cm
Electronic and Fitted (corrected) bandgap	6.94 eV and 10.27 eV
Bandgap type	Insulator indirect gap

3. Experimental Methods and Materials

The investigation of wide gap crystals carried within this master thesis is purely experimental research. I myself accomplished in cathodoluminescence experiments in Tartu, whereas synchrotron radiation research at MAX IV Lab in Lund, Sweden, was performed either by colleagues from our research team or even by the FinEstBeAMS beamline staff because of limited lab access due to a pandemic. In this section, a general comparison of both luminescence spectroscopy methods used will be given.

Cathodoluminescence is a widely used experimental method used in luminescence studies of wide gap crystals. An electron beam, pulsed or stationary, is used to excite materials under investigation. Typically, a few keV electron beams are used in such experiments, which allow investigating luminescence in a full transparency range of materials extending from infrared to VUV, being limited by the energy gap value of the material. It is a powerful method to study radiative processes with a low quantum yield. Its drawbacks are sample charging in the case of insulators and radiation damage due to energetic particles. Both may alter luminescence intensity making data analysis more complicated. Its selectivity is not so high because primary electron beams result in the creation of low energy secondary electrons, which basically can excite all possible levels. Thus, it is not well suited for the identification of particular excitation mechanisms, but it provides a complementary research method to the luminescence studies under synchrotron radiation excitation.

Synchrotron radiation (SR) is electromagnetic radiation, which is emitted when the relativistic charged particles are moving with the acceleration in the magnet lattice of a storage ring. Depending on the particle energy storage rings cover a wide spectral range extending from the infrared to X-Ray region. Moreover, SR is among the brightest light sources, which provide pulsed and polarized radiation with continuous tuneability. An inherent well-defined time structure of SR is due that electrons (used in Lund) in the storage ring are assembled in bunches and not distributed continuously in their orbit. Fig. 9, demonstrates how the time structure of photon pulses is formed due to the electrons emitting in bunches. In a single bunch mode, the storage ring is filled just with one bunch and in the 1.5 GeV storage ring at MAX IV the respective time interval (Δt) between subsequent light pulses is as large as 320 ns, whereas the width of the pulse is ~160-180 ps.

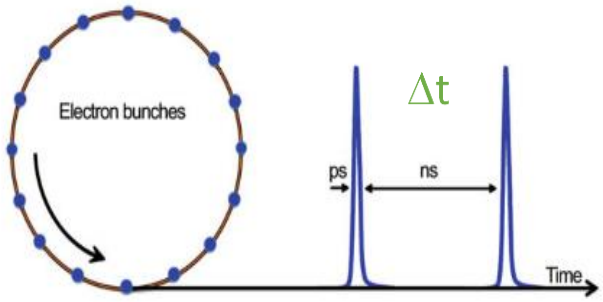

Fig. 9. Time structure of emitted radiation pulses. Photon pulses of a few hundred ps width (FWHM) are separated by a few hundred ns intervals (Dt) in the single bunch operation mode. Courtesy of V. Pankratov.

The magnets of modern storage rings keep the electron bunches well-focused, resulting in a rather small source size emitting photons into a narrow spatial cone. Thus, the obtained light beam can be smoothly directed by the beamline optics resulting in a small focal spot on the sample. The inherent time structure together with the tuneability of SR and its small spot size makes it particularly well suited for time-resolved luminescence spectroscopy in a wide photon energy range.

3.1 Cathodoluminescence setup

Cathodoluminescence (CLU) technique allows them conveniently to study all kinds types of emissions (intrinsic or extrinsic) independently of their origin because the energetic keV electron beam populates highly excited states, which may decay to all available relaxation channels of electronic excitations. There is a possibility to adjust the energy of the electron beam providing a direct control on the penetration depth of the exciting particles. Thus, one can study luminescence either from the bulk or from the layers close to the surface. For this purpose, an experimental setup for cathodoluminescence, which allows to carry out such studies in wide spectral and temperature range, has been constructed [31]. It is continuously developed further according to research needs and the latest description can be found below.

The low-temperature cathodoluminescence studies were carried out using the home-built set up in the Institute of Physics in Tartu (Fig. 10). It allows studying luminescence phenomena in a wide range of temperatures (5 – 400 K) under steady and pulsed 10 keV electron beam excitation [31]. The low temperature is achieved by using a closed-cycle vacuum cryostat (Advanced Research Systems) and controlled by the Lake Shore 331 thermo-controller. The setup is equipped with two monochromators, allowing for simultaneous recording of emission spectra in the UV-Vis and VUV range. The emission spectra in the UV-Vis range (6 – 1.8 eV) were recorded through a grating ARC Spectra Pro 2300i monochromator equipped with a Hamamatsu photon counting head H8259. The typical spectral resolution was as high as 0.5 nm for the UV-Vis range. The spectra in the VUV range were recorded with a custom-built double monochromator with 0.64 nm resolution using a solar-blind photomultiplier Hamamatsu R6836. All necessary corrections for the transmission of monochromators and the detector sensitivity were applied. An electron gun (EGG-3101 Kimball Physics), which operates in the energy range up to 10 keV, is used to excite the sample under investigation.

In this research, it was used in both operation modes either providing the steady or pulsed (repetition rate 5 kHz, pulse width 10 ns) excitation. In the steady mode, the system can be used to irradiate samples with the electron beam for a given dose. Thereafter, phosphorescence or thermo-stimulated luminescence registration from samples is possible. It can be done by simultaneous registering of a spectrally integrated (a separate PMT tube covering 1.8-6 eV range) signal together with recording emission spectra during heating.

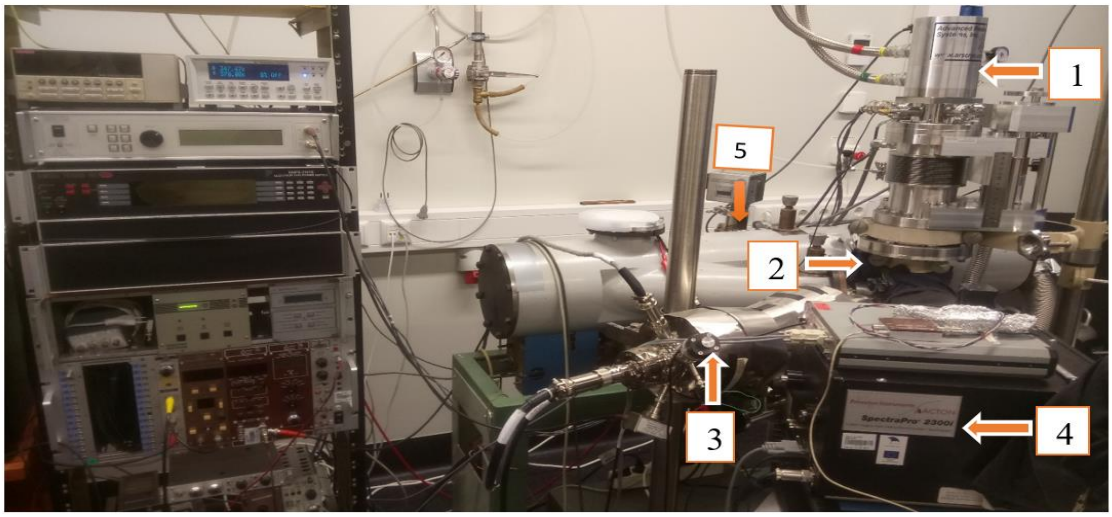

Fig. 10. Photo of Cathodoluminescence setup. (1) a closed cycle vacuum cryostat (Advanced Research Systems); (2) Vacuum chamber ≈ 10^{-7}Torr; (3) An electron gun (EGG-3101 Kimball Physics); (4) ARC Spectra Pro 2300i spectrometer for the UV-visible range; (5) a home-built VUV monochromator. The components of the CL setup are designated by numbers on the photo.

3.2 Luminescence setup at the FinEstBeAMS beamline of the MAX IV laboratory

The FinEstBeAMS beamline for atmospheric and materials science is located at the 1.5 GeV storage ring of the MAX IV synchrotron radiation laboratory in Lund, Sweden. It is the first international beamline of the MAX IV lab, which was jointly funded by the Finnish and Estonians investments and was constructed and built by the consortium of Estonian (University of Tartu) and Finnish Universities (the University of Oulu, University of Turku, University of Tampere) together with MAX IV Lab. It is in the operation since 2018 after the initial commissioning was completed.

FinEstBeAMS is a high brilliance ($1x10^{11}$ - $8x10^{13}$ ph/s) beamline, where an elliptically polarizing undulator as the radiation source provides photons in the UV to soft X-ray range 4.5 – 1300 eV [32]. The primary is a monochromator equipped with two plane gratings – 92 l/mm (4.5 – 50 eV, used in all measurements in this study) and 600 l/mm (15 – 1300 eV), operating in grazing incidence geometry. An ellipsoidal mirror M4a focuses the photon beam to a 100 x 100 µm spot on the samples mounted on a cold finger of a closed-cycle He cryostat mounted in a chamber providing ultra-high vacuum conditions. The layout of the beamline is shown in Fig. 11.

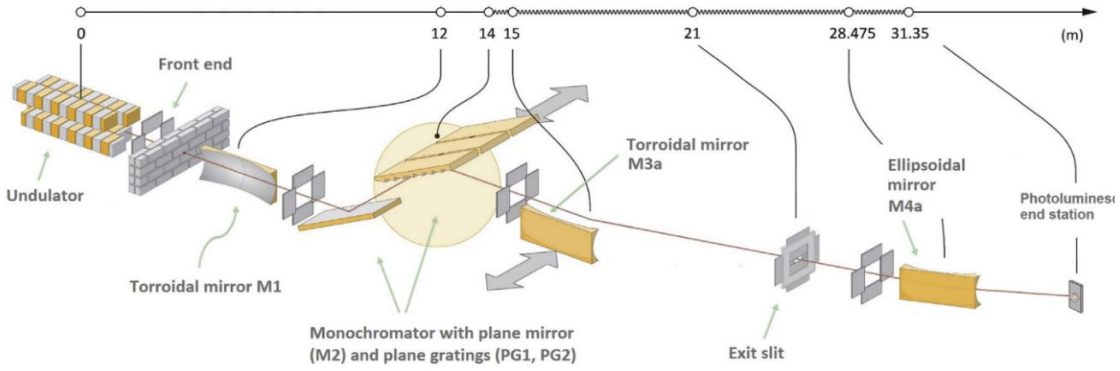

Fig. 11. The optical layout of the FinEstBeAMS beamline with the photoluminescence end station [32].

Low-temperature time-resolved and time-integrated luminescence studies of BaY_2F_8 and KY_3F_{10} single crystals in VUV were performed using a photoluminescence (PL) end station mounted in one of the branch-lines at FinEstBeAMS (Fig. 12) The luminescence is collected in the experimental chamber using a fiber optic cable (~2 m in length) connected to a 0.3 m Andor Shamrock SR-303i spectrometer, which is used for the analysis of photoluminescence. The spectral analysis is carried out either with an Andor CCD camera (Newton DU970P-BVF) or a Hamamatsu photon counting head H8259-01. The latter detector covers the spectral range of 200 – 900 nm. Implementation of the fiber optic cable connection results in significantly reduced luminescence intensity at wavelengths below 250 nm. This also creates difficulties in acquiring reliable calibration lamp spectra, which are required for correcting recorded emission spectra to the spectral sensitivity of the PL setup in this spectral region. For this reason, the emission spectra recorded at the PL end station in the wavelength scale are presented as measured. The typical spectral resolution used in the recording of the luminescence spectra was 9.7 nm.

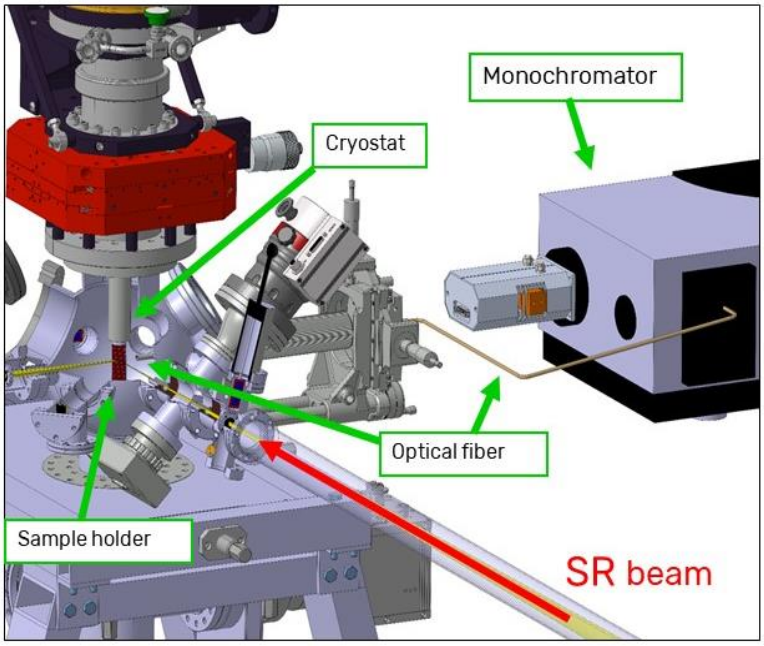

Fig. 12 A scheme of the photoluminescence end station at FinEstBeAMS [32].

Along with time-integrated luminescence spectra also the luminescence decay curves, time-resolved emission, and excitation spectra were recorded using a single bunch operation mode with parameters described in section 3. For such measurements, an ultra-fast Hamamatsu R3809U-50 MCP-PMT was used. The MCP-PMT signals were processed by an ORTEC 9327 constant fraction discriminator and timed by a Chronologic xTDC4 time-to-digital converter with the 13 ps bin width. The elaborated advanced technical hardware and software solution by our research group is based on the modern xTDC4 device allowed to detect more than one photon per excitation pulse using time stamping of the arrival of multiple photons the whole-time interval of 320 ns. Thus, the modern TDC opens new possibilities of a signal recording as discussed above and the data analysis performed later can target fast and slow relaxation processes by choosing the respective time windows in the recorded emission and excitation spectra. An instrumental response function (IRF) with a temporal resolution of 180 ps was achieved in the present experiments.

Special care was taken to suppress higher-order radiation causing a particular problem in the grazing incidence geometry together with an undulator source. Higher harmonic radiation generated by the undulator is always present and it can pass through the primary monochromator in the second order of selected energy. This is a serious problem for luminescence studies because the higher-order excitation results in a similar emission spectrum without any possibility to discriminate the influence of such disturbing high-energy photons. In the case of the FinEstBeAMS, there is a set of thin metal filters (In, Sn, Mg, Al), and classical optical windows made of fused silica and MgF_2 are available to handle the problem described. But this solves the higher-order suppression problem only partially because not the whole energy range understudy is conveniently covered with suitable filters. Also, the transmission of these filters mounted in the beamline varies from a few to tens of percent. Thus, special care has to be taken in order to create trustworthy excitation spectra in the entire photon energy range 4.5 – 50 eV studied.

The photon flux of the beamline is recorded with an AXUV-100G photodiode placed before the sample holder. Its signal is corrected to the standard quantum efficiency curve of such photodiodes and thereafter used to process the excitation spectra by normalizing to the same amount of incident photons. In our experiments, a typical slit width of the primary monochromator was in the range 50-250 μm, which corresponds to the spectral resolution

better than 11 meV at 20 eV. The degradation of samples investigated at FinEstBeAMS may also occur under such high photon flux, therefore the excitation density conditions are to be properly accounted for by researchers.

3.3 BaY_2F_8 and KY_3F_{10} single crystals

In this work, high-quality BaY_2F_8 and KY_3F_{10} single crystals were investigated provided by crystal growth laboratories in Russia. BaY_2F_8 crystals were grown by the vertical Bridgman method as described in this publication [33]. KY_3F_{10} crystals were synthesized using the hydrothermal synthesis technique described in [34]. No further characterization of the composition and crystal structure for studied crystals was performed in this work. The visually transparent single crystal pieces of a few mm size were studied. It is well known that Y-containing compounds have rare earth impurities in few ppm levels in their composition.

4. Results

4.1 Cathodoluminescence spectra of BaY_2F_8 and KY_3F_{10}

Fig. 13. (a) demonstrates the cathodoluminescence spectra of BaY_2F_8 single crystal at 5.2 K. It is recorded through two different spectrometers (VUV monochromator and UV-Visible spectrometer) with two different detectors. Therefore, the experimental data corrected to the spectral sensitivity is presented in two independent intensity scales for better visibility. The major luminescence peak is at 4.5 eV and it is due to self-trapped exciton emission [10]. The weak luminescence extending to the VUV spectral range (the right-hand intensity scale) is due to cross-luminescence. The cathodoluminescence study of wide-gap insulators is complicated due to the charging problem of crystals and sometimes it prohibits high-quality measurements. It is obvious that it would be very difficult to identify the high-energy edge of cross-luminescence from the VUV spectrum depicted in Fig. 13(a). In Fig. 13. (b), luminescence spectra of the BaY_2F_8 single crystal at 10 K excited by 90 eV photons at the BW3 beamline (DORIS, DESY) are shown [13]. The time-integrated luminescence spectrum resembles that one obtained under 10 keV e-beam excitation with the monotonously falling intensity towards VUV. The time-resolved spectra, recorded in the time window with delay δt=0.1 ns and with Δt=1.6 ns shows a well-pronounced onset at 7.6 eV and are assigned to the high energy edge of cross-luminescence. In the cathodoluminescence spectra Fig. 13 (a), there is also a faint feature at the same energy indicating a possible cross-luminescence edge in BaY_2F_8.

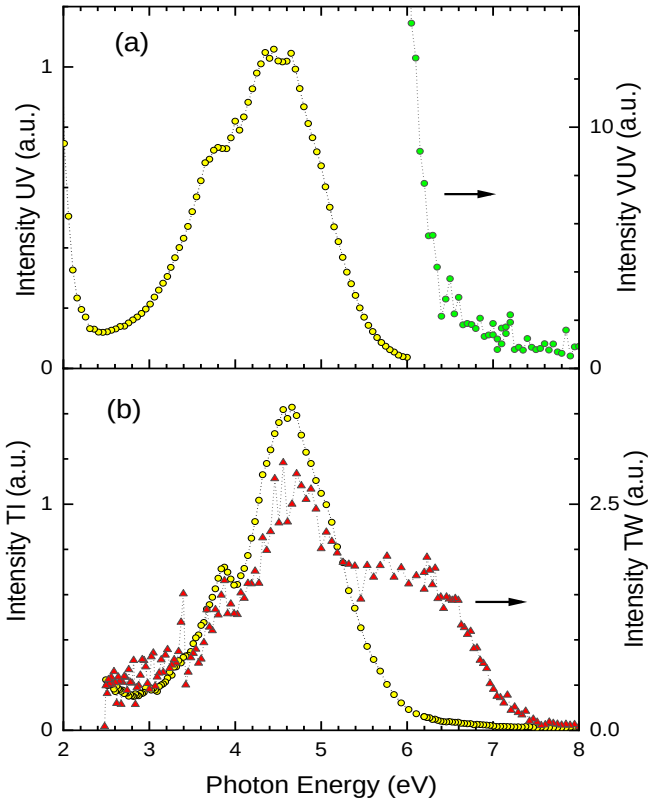

Fig. 13. (a) Cathodoluminescence spectra of BaY_2F_8 single crystal at 5.2 K excited by 10 keV electron beam. (b) Time resolved luminescence spectra of BaY_2F_8 single crystal at 10 K excited by 90 eV photons at the BW3 beamline of DORIS at DESY [13] o symbols designate time integrated emission spectra and Δ symbols recorded in the time window delayed 0.1 ns and with a length of 1.6 ns [32].

Fig. 14 shows cathodoluminescence spectra for KY_3F_{10} single crystals at various temperatures. In VUV the emission extends to 9.2 eV, where its high energy onset is well identified and the emission can be assigned to cross-luminescence. In the UV-visible region, cathodoluminescence has a more complex structure. It was found that in different experiments relative intensities of the main features may vary as shown for the emission bands peaked at 4.5 and 3.2 eV. It indicates that single-crystal samples may have inhomogeneous regions, where sample composition is different. In the room temperature spectrum, narrow emissions lines are visible (from 4.5 eV to the lower energies), which are assigned to rare earth impurity ions. The strongest emission line of this impurity is at 2 eV and it is present at 300 and 5 K.

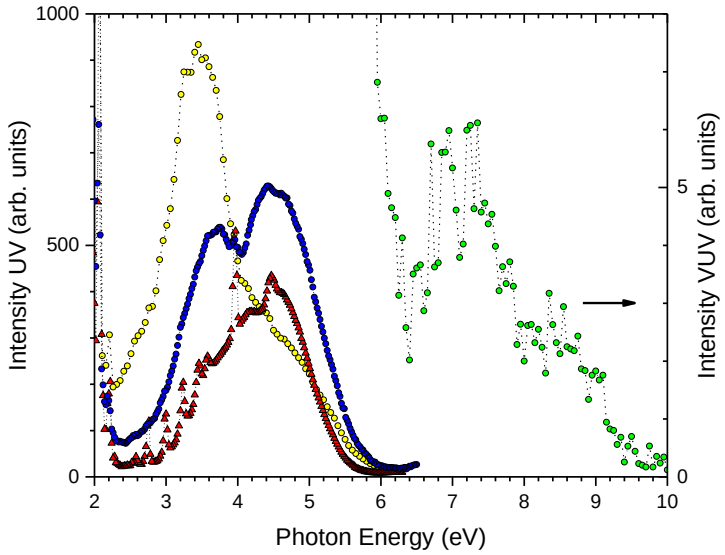

Fig. 14. Cathodoluminescence spectra of KY_3F_{10} single crystals at 5 K (filled symbols o) and 300 K (red Δ) excited by 10 keV electron beam. The spectra recorded in VUV (green o) and UV (yellow o) were obtained in the same experiment. Room temperature (red Δ) and low temperature UV spectrum (blue o) were recorded in another experimental session.

4.2 Photoluminescence spectra of BaY_2F_8 under VUV excitation

Due to the wide bandgap, experimental studies of fluorides were carried out in the VUV region. Such studies were performed using the photoluminescence setup at the FinEstBeAMS beamline at the MAX IV Laboratory. The emission spectra in the UV-visible and their excitation spectra were studied under selective excitation by photons up to 45 eV in VUV. Fig. 15 shows luminescence spectra of the BaY_2F_8 single crystal at 6.6 K. The broadband emission peaked at 4.3 eV is the dominating feature under excitation by 10 eV photons (Fig. 15 (a)). At the low energy side of the main emission band, starting from 3.6 eV narrow emission lines are visible. This is resulting from the 4f-4f emissions due to rare earth impurities at low concentration. In Fig. 15(b) luminescence spectra of the BaY_2F_8 single crystal at 6.6 K excited by 45 eV. The maximum of the main emission band is shifted to 4.6 eV and the asymmetric shape indicates that it is non-elementary.

At 295 K luminescence spectra resemble those recorded at 6.6 K. The excitation by 9.75 eV photons results in two broad emission bands peaked at 4.3 and 3.7 eV as shown in Fig. 15 (c).

An increase of photon energy to 45 eV, provides the appearance of the high energy wing in the emission spectrum, which extends to VUV (Fig. 15 (a)). Its possible origin will be discussed later.

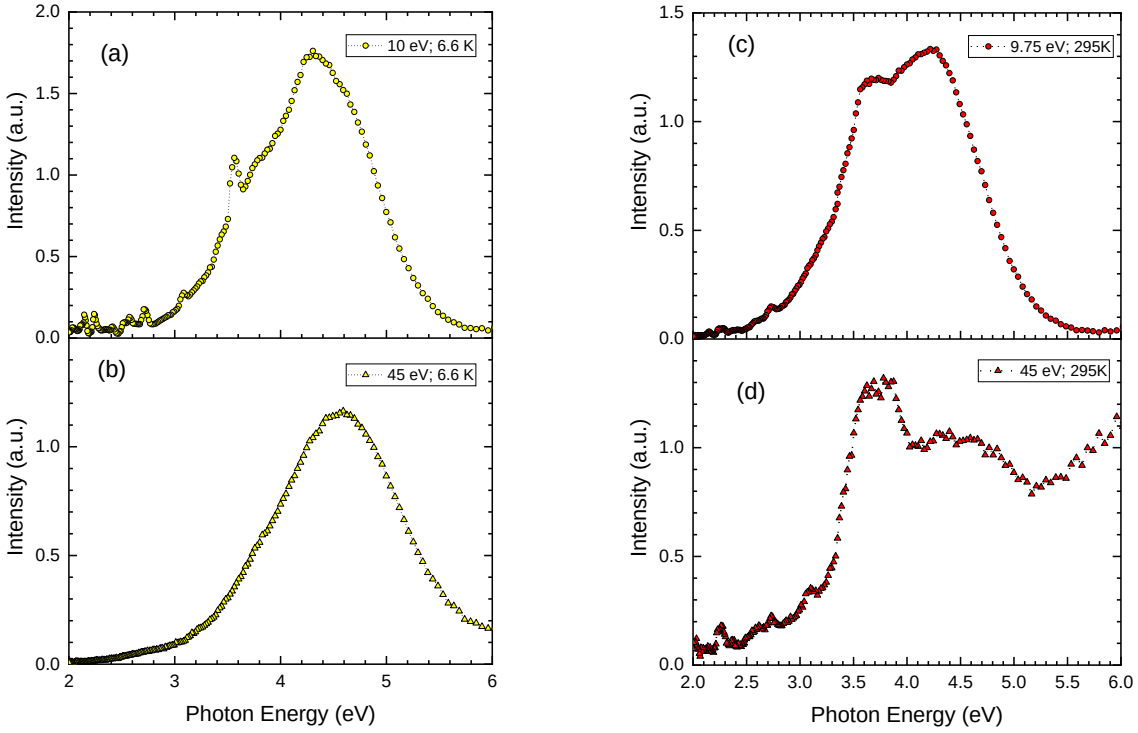

Fig. 15. Time-integrated photoluminescence emission spectra excited by 10 eV (a) and 45 eV (b) photons of a BaY_2F_8 crystal at 6.6 K, and by 9.75 eV (c) and 45 eV (d) at 295 K.

Time-integrated photoluminescence excitation spectra for UV emissions for BaY_2F_8 crystal at various temperatures are shown in Fig. 16. The strongest excitation peaks are found near 10 eV, showing the onset of intrinsic absorption for BaY_2F_8. Above this peak at higher energies, there are some features in the excitation spectrum of the 4.96 eV emission at 6.6 K (Fig. 16 a), whereas at 295 K the main feature for the 4.77 eV emission in the excitation spectrum is near 20 eV as shown in Fig. 16 (c).

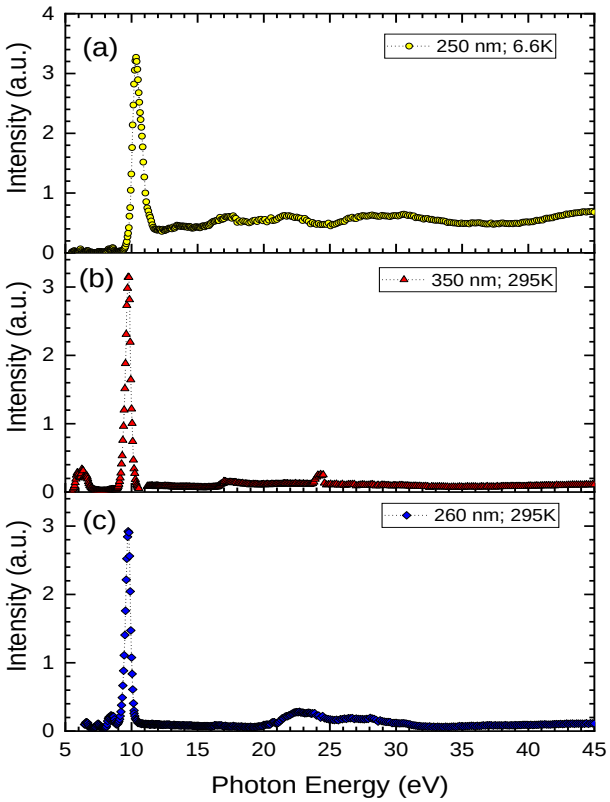

Fig. 16. Time-integrated photoluminescence excitation spectra of BaY_2F_8 crystal at 295 K and 6.6 K. It is recorded for 4.96 eV (a, yellow symbols) at 6.6 K, 3.54 eV (b, red symbols) and for 4.77 eV (c, blue symbols) emissions at 295 K. The intensities of the spectra have been scaled for better visualization.

4.3 Photoluminescence spectra of KY_3F_{10} under VUV excitation

Emission spectra of KY_3F_{10} crystal at various temperatures and excitation conditions are shown in Fig. 17. Under excitation at low energies (Fig. 17 (a) and (b)), the main broad emission band is peaked at 4.8 eV at 295 K, it is shifted to lower energy with a maximum at 4.5 eV. From the FWHM of the emission band, it is obvious that several emission centers contribute to its formation. The narrow bands (from 4 eV towards lower energies), revealed at 295 K, are due to the 4f-4f emissions (Fig. 17 (b)). Independently of the sample temperature the same line structure is also clearly visible under excitation by 45 eV, (Fig. 17 (d)). The emission spectra at 295 K practically coincide in shape. The same KY_3F_{10} single crystal was studied during

several experimental sessions and results under 45 eV excitation are shown in Fig. 17 (c). The discrepancy of the shapes is assigned to the fact that emission from two different spots on the crystal surface was recorded. The recorded spectra shown in Fig. 17 (c) do not contradict each other because the ratio of the two emission bands peaked at 5.0 and 3.5 eV changes. As a result, these peaks appear as high (yellow symbols) or low energy (blue symbols) shoulders in the recorded curve (Fig. 17 (c)).

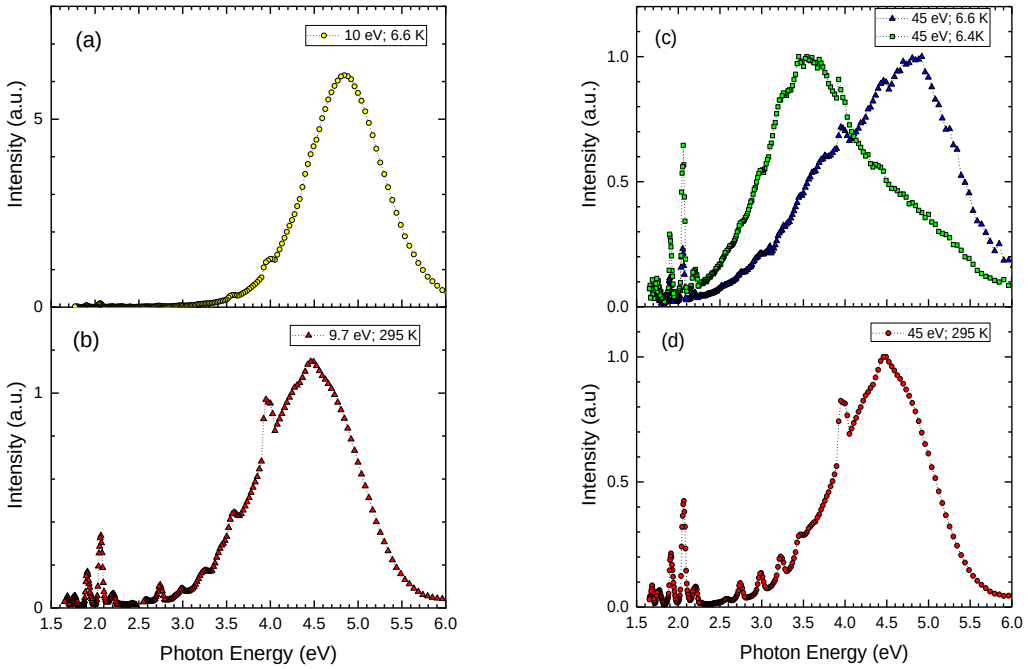

Fig. 17. Time-integrated photoluminescence emission spectra excited by 10 eV (a), 9.7 eV (b) and 45 eV (c, d) photons of a KY_3F_{10} crystal at 6.6 K (a, c) and 295K (b, d).

The low-temperature excitation spectra for various emissions from KY_3F_{10} single crystal are shown in Fig. 18. The excitation spectrum for the 2.07 eV emission has all features at photon energies below 10 eV (Fig. 18. (a)). The 3.35 eV emission has low-intensity spectral features below 10 eV, which are followed by a stronger maximum at 10.3 eV and the most prominent excitation peak at 10.95 eV. The UV emission at 4.5 eV has the most intense excitation maximum at 9.9 eV, which is followed by the next peak at 10.9 eV. At higher energies above 15 eV, there are broad excitation bands observed up to 35 eV.

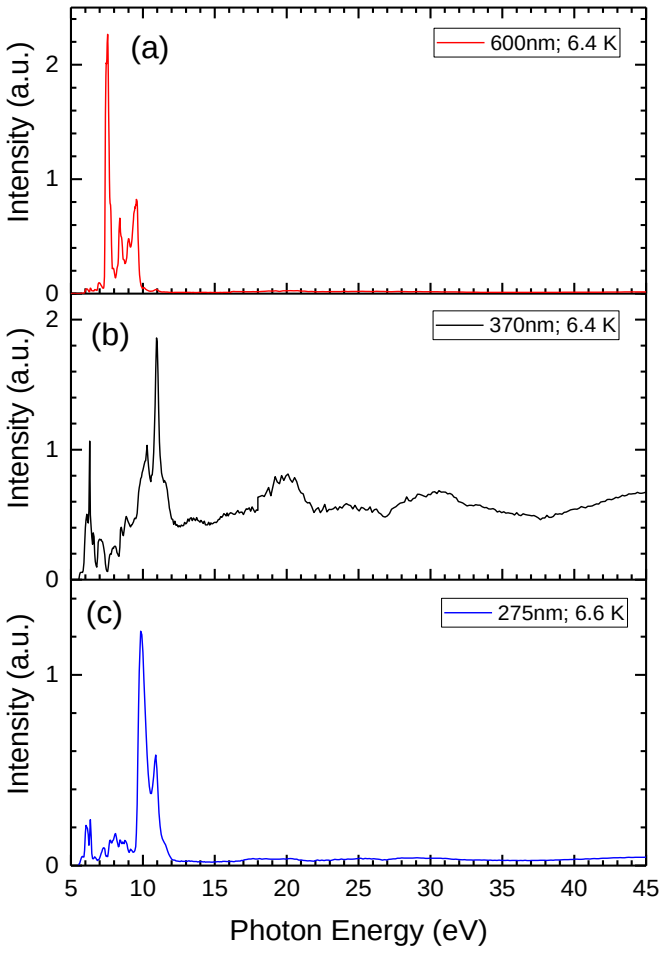

Fig. 18. Time-integrated photoluminescence excitation spectra of KY_3F_{10} crystal, recorded at 6.6 K and 6.4 K: (a) 2.07 eV (a, red line), (b) 3.35 eV (b, black line), and (c) 4.50 eV (c, blue line) emissions. The intensities of the spectra have been scaled for better visualization.

5. Discussion

The results presented above show that for both single crystals BaY_2F_8 and KY_3F_{10} possess very complex luminescence spectra consisting of intrinsic emissions like cross-luminescence (CL) and that of self-trapped excitons (STE), along with extrinsic ones due to rare earth and other impurities. It is obvious that all possible experimental methods (incl. time resolved luminescence techniques) have to be used in order to determine the nature of various emissions and electronic band structure parameters and how to distinguish spectrally overlapping emissions to be able to analyze relaxation processes of electronic excitations. Understanding all these phenomena helps to use materials with cross-luminescence in various detector applications and to have a deeper understanding of the properties of wide-gap materials.

5.1 Luminescence and electronic properties of BaY_2F_8 single crystal

In order to separate various kinds of emissions, the time-resolved luminescence spectroscopy was applied at the FinEstBeAMS beamline in Lund. The decay curve (blue line) of cross-luminescence recorded at 4.82 eV, which was excited by 20-30 eV photons during an excitation scan, is shown in Fig. 19. for BaY_2F_8 single crystal at 7 K. The red curve is the instrumental response function (IRF), which characterizes time resolution achieved in these experiments using a single bunch operation regime. The obtained IRF value FWHM was as good as 180 ps.

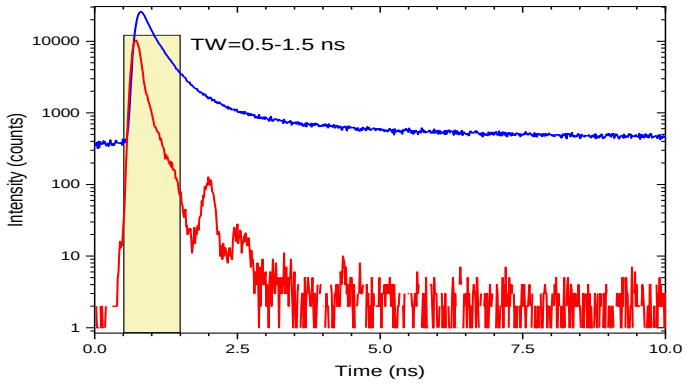

Fig. 19. Decay curve (blue line) for luminescence at 4.82 eV recorded through interference filter (257 ± 20 nm) under excitation by 20-30 eV photons from the BaY_2F_8 crystal at 7 K. In order to have statistically high-quality data the decay was recorded during the excitation scan from 20- 30 eV. An instrumental response function is also shown (red line). The box in the figure shows a time window (TW), which is shifted by δt=0.5 ns and with a length of Δt=1.0 ns used in the analysis of time resolved excitation spectra.

The decay was analyzed by fitting experimental data with the multi-exponential decay function. In the fast decay part, three components were obtained: τ_1=110 ps (45 % of initial amplitude intensity); τ_2=430 ps (39 %), and τ_3=5 ns (16 %). There is also the strong background of slower emission with μs lifetime and it cannot be studied at the small 1.5 GeV storage ring, where electron bunches are separated by 320 ns time interval in a single bunch mode. The fastest component is partially assigned to the contribution of the scattered exciting radiation, being always present in any decay measurement under a powerful excitation source. Since decay curves were recorded through the inference filter before the MCP-PMT mounted on the quartz window of the experimental chamber, such contribution is expected to be stronger than recording through a monochromator. Such decay times are typical for cross-luminescence. Initial studies in the 1990s have revealed that for the BaY_2F_8 host the decay time τ is estimated to be either ~3 ns [10] or τ_1 = 0.64 and τ_2 =1.35 ns in two exponential approaches [14]. The decay times revealed in this study are a bit shorter, but they are in the same agreement with earlier studies.

Time-resolved luminescence spectroscopy opens new possibilities for the analysis of complicated emission spectra. Such an example is presented in Fig. 20, where the time-integrated emission spectrum is shown together with those analyzed in various time windows selected after recording spectral dependence of luminescence decays either every emission wavelength or excitation energy, respectively. In Fig. 19 the box represents the time window (TW) used in the analysis of excitation spectra of BaY_2F_8 crystal. It is delayed by δt=0.5 ns and has a length of Δt=1.0 ns. Analogous emission spectra in time windows are shown in Fig. 20.

Time integrated emission spectrum recorded at 7 K has a maximum at 4.5 eV in agreement with data presented in Fig. 15. (b). The cross-luminescence extends to the VUV region (see Fig. 13) and is pronounced here as shoulder till 6 eV, which is an experimental detection limit of luminescence setup at FinEstBeAMS. Time resolved luminescence spectra, which were recorded in order to discriminate intrinsic STE emission being practically quenched at 300 K [10], give more information on the nature of emissions in BaY_2F_8. Emission spectra recorded in two fast time windows (δt_1=0 and Δt_1=10 ns, δt_2=0 and Δt_2=50 ns) show intensity increase towards 6 eV due to contribution of cross-luminescence. On the low energy side, the limit is near 3 eV, but it can be that the emissions with a longer lifetime give their contribution in these

time windows and it does not belong to CL in the whole range. The third long TW (δt_3=50 and Δt_3=250 ns) shows that there is an emission center with a luminescence maximum at 3.8 eV, which is assigned to the defect or impurity center. The luminescence spectra recorded are in good agreement with those studied before [10].

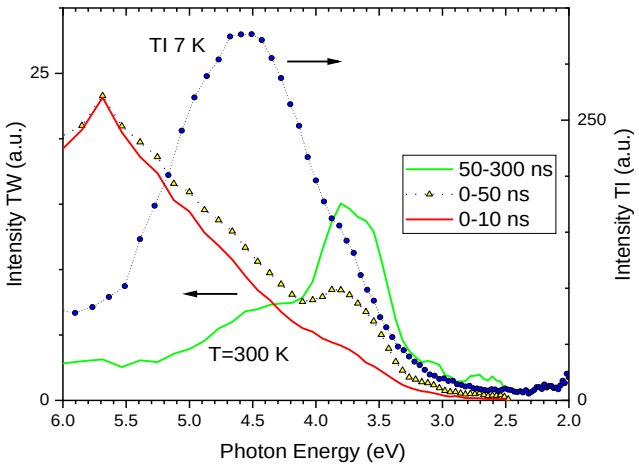

Fig. 20. Time integrated emission spectrum of BaY_2F_8 crystal at 7 K excited by 45 eV photons (blue symbols). Time resolved emission spectra of BaY_2F_8 crystal at 300 K excited by 45 eV photons recorded in the time windows: δt=0 and Δt=10 ns (red line), δt=0 and Δt=50 ns (yellow symbols), δt=50 and Δt=250 ns (green line).

The same time window approach was applied in the analysis of the excitation spectra to reveal the cross-luminescence excitation onset E_{gc} due to ionization of Ba 5p core level. As shown in Fig. 16 (c), at 295 K this onset near 19 eV can be distinguished because STE emission is thermally quenched. At low temperatures, this feature is masked due to the strong contribution of the STE emission, which is well excited in the fundamental absorption.

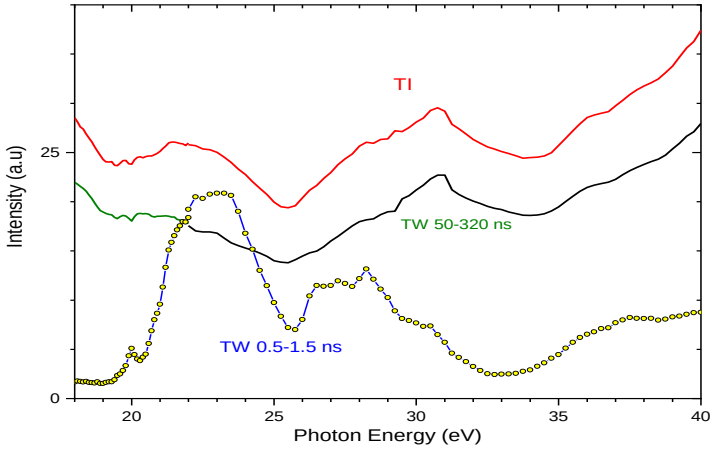

Fig. 21. Excitation spectra for luminescence at 4.82 eV recorded through interference filter (257 ± 20 nm) of BaY_2F_8 crystal at 7 K. The time integrated excitation spectrum is designated with a red line, spectra in time windows are shown by yellow symbols (δt=0.5 and Δt=1 ns) and by green line (δt=50 and Δt=270 ns), respectively.

Fig. 21. shows the excitation spectra recorded for luminescence at 4.82 eV (recorded through interference filter 257 ± 20 nm) of BaY_2F_8 crystal at 7 K. The spectral features in TI and long TW spectra do not show any clear onset, which can be related to the ionization of the Ba 5p core level. The excitation spectrum in a short time window has a distinct rise of excitation efficiency at E_{gc}=19.3 eV and structures following at higher energies are due to the interband transitions from the Ba 5p states. This is in good agreement with already the published value of early studies [12].

The excitation spectra recorded for UV emissions at 4.96 and 3.87 eV at 6.6 K (4.77 and 3.54 at 295 K) near the fundamental absorption edge of BaY_2F_8 are shown in Fig. 21. At 295 K the excitation peak for both emissions is at 9.75 eV, whereas for 4.96 eV emission is peaked at 10.35 eV and for 3.87 eV emission it is at 10.2 eV. Since 4.96 eV is due to self-trapped excitons, these excitation features are assigned to exciton formation E_{exc}. This value is below that reported in the literature for E_{exc}=11.4 eV [10] or 11.7 eV [12] and the corresponding energy gap value was estimated to be E_g=12.4 eV [12]. Analogously to the Ref. [35], E_g value can be estimated from the excitation spectra. Using data presented in Fig.22 the deduced E_g has a smaller value $E_g \sim 11.4$ eV.

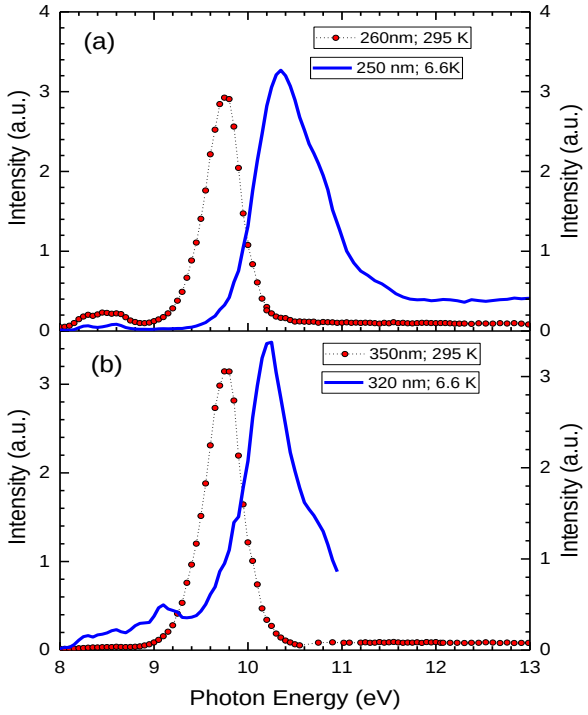

Fig. 22. Excitation spectra for luminescence recorded from BaY_2F_8 crystal at 4.96 and 3.87 eV at 6.6 K; and 4.77 and 3.54 at 295 K. The higher energy UV emission is designated by blue lines and lower energy one with symbols.

The electronic band structure for BaY_2F_8 from the Materials studio database is depicted in Fig. 4. Only the calculation for the F 2p valence and conduction band states is available, which does not allow to compare the position of the Ba 5p core level with the experimental results. The determined values of $E_g \sim 11.4$ eV and $E_{gc}=19.3$ eV positions Ba 5p core level 7.9 eV below the top of the valence band. The respective value for BaF_2 is 8 eV, showing that the position of core levels is practically independent of the chemical composition and structure of the substance. This value of 7.9 eV is in good agreement with the high energy edge of the cross-luminescence spectrum at 7.6 eV (see Fig. 13.). According to theoretical calculations, the width of the valence band is ~2.5 eV, thus one can expect that the low energy edge of cross-luminescence is near 5.1 eV. Comparing luminescence spectra shown in Figs.13(b), 15(d), and 20 one can see that there are always changes near 5.0 eV. This is the region where STE emission peaked at 4.6 eV (Fig. 15(d)) starts to overlap with cross luminescence.

5.2 Luminescence and electronic properties of KY_3F_{10} single crystal

According to published literature, there is practically no data reported on the luminescence properties of KY_3F_{10}. However, some other K-based ternary fluorides have been studied under soft X-ray excitation at room temperature in the UV-VUV region (Fig. 7).

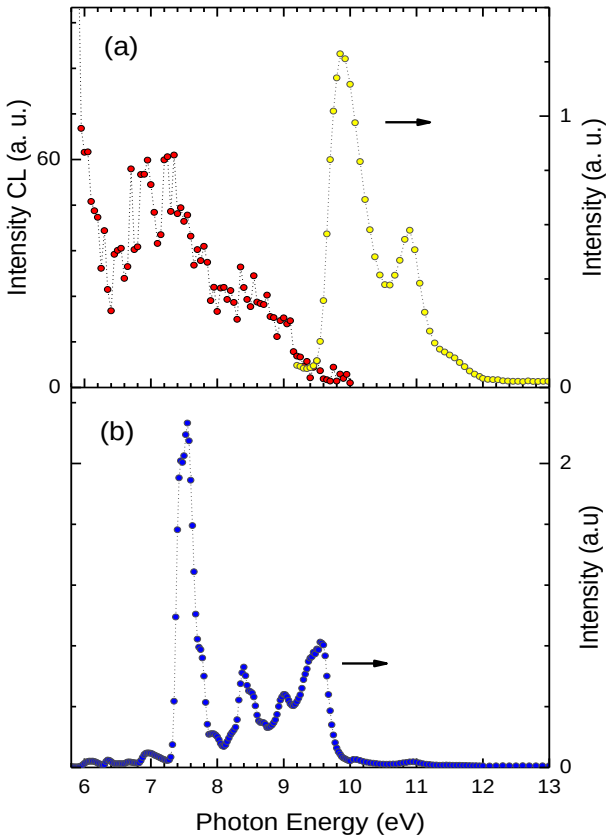

Fig. 23 (a) TI cathodoluminescence spectrum of KY_3F_{10} crystal at 7 K excited by 10 keV electron beam (red symbols). The excitation spectrum for 4.5 eV emission recorded at 6.4 K (yellow symbols). (b) The excitation spectrum for 2.07 eV emission recorded at 6.4 K (blue symbols).

Analogously to other K-F based the cross-luminescence in KY_3F_{10} is expected to extend to the VUV region. Cathodoluminescence spectrum (red symbols), depicted in Fig. 23 (a), covers spectral range practically to the intrinsic absorption as shown in the same graph by the excitation spectrum of 4.5 eV emission. The excitation peak at 9.9 eV is assigned to the creation of excitons E_{exc}. The minimum between two excitation peaks at ~ 10.6 eV is due

to strong exciton absorption peak decreasing the penetration depth into the crystal and thus the energy gap value is located on the high energy side of the second excitation peak, resulting in $E_g \sim 11.4$ eV. The latter value has been reported for KYF_4 in Ref. [27]. Fig. 23 (b) shows the excitation spectrum for 2.07 eV emission, which is due to the small amount of rare earth impurity introduced during the growth of KY_3F_{10} single crystal. This impurity can reabsorb cross-luminescence and modulate cross-luminescence spectrum by the appearance of minima as shown in Fig. 23. (a).

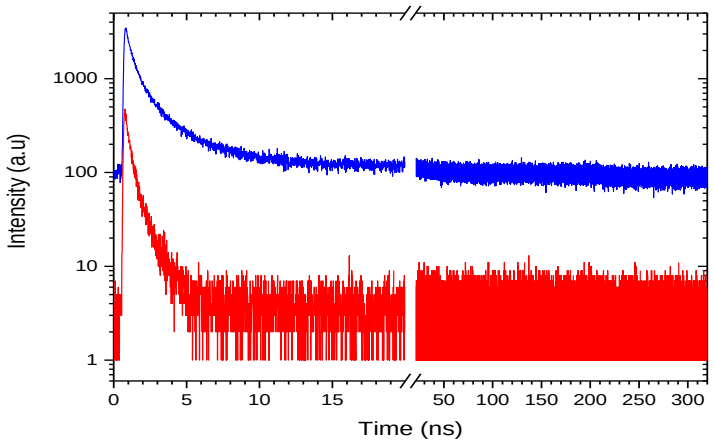

Fig. 24 Decay curve (blue line) for luminescence at 4.82 eV recorded through interference filter (257 ± 20 nm) under excitation by 45 eV photons from the KY_3F_{10} crystal at 7 K. Decay curve (red line) for luminescence at 5.74 eV recorded through interference filter (216 ± 20 nm) under excitation by 45 eV photons from the KYF_4 crystal at 7 K.

The decays, shown in Fig. 24, were analyzed by fitting the experimental data from KY_3F_{10} single crystal with the multi-exponential decay function including a deconvolution by the instrumental response function recorded in the identical conditions through the same IF-filter and the scattered exciting light from the sample holder. In the fast decay part, three components were identified: τ_1=45 ps (71 % of initial amplitude intensity); τ_2=625 ps (23 %), and τ_3=3.27 ns (5 %). There is also the strong background of slower emission with the μs lifetime and it cannot be studied at the 1.5 GeV storage ring with a small circumference. But the fitting procedure found a τ_3=274 ns (0.3 %) component, which can be expected since through the IF bandwidth different kinds of intrinsic and extrinsic emissions can be detected. The fastest

component is partially assigned to the contribution of the scattered exciting radiation, as discussed for BaY_2F_8 in section 5.1.

The decomposition of the second decay of KYF_4 crystal, shown in Fig. 23, resulted in three exponential functions with the following parameters: τ_1=156 ps (82 % of initial amplitude intensity); τ_2=878 ps (17.9 %), and a minor contribution τ_3=84 ns (0.1 %). Such sub-nanosecond decay times are typical for cross-luminescence. It is important to note that there is nearly no slow background with the μs lifetime, which points to the fact that STE emission can be found at lower energies. The decays of KY_3F_{10} in the UV region were analyzed for the first time and there is no literature data. A recent publication reports that cross-luminescence at 8 eV in KYF_4 single crystal has the decay time τ~1.1 ns [36], which is comparable with the results of the present work. The decay times revealed that this study has a tendency to be shorter than reported in the earlier studies, but this is a subject for future studies.

Time integrated emission and excitation spectra recorded from KY_3F_{10} single crystal at various temperatures are shown in Fig. 24. At 295 K, the emission spectra have the main maximum at 4.5 eV in agreement with the cathodoluminescence spectrum shown in Fig. 14 and photoluminescence spectra at Fig. 17 (b, d). The contribution from rare-earth impurities is revealed as a set of narrow emission lines at lower energies present at both excitation energies and in all temperatures. It shows that there the host to impurity energy transfer takes place. At 6.6 K The broad emission bands observed have the main maximum at 3.6 eV, followed by shoulder at 5 eV. It is in the agreement with cathodoluminescence spectra presented in Fig. 14, where the maxima of emissions were depending on the excitation spot on the KY_3F_{10} single crystal. Under excitation by 26 eV photons, there is a noticeable increase of luminescence intensity from 5.5 eV towards VUV. The excitation spectra have broad features in the energy.

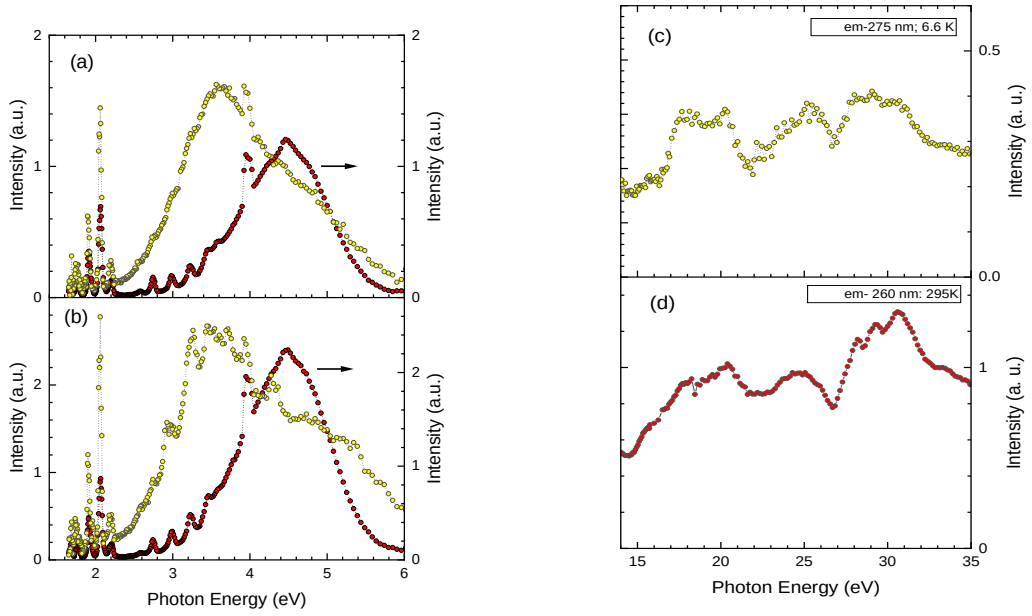

Fig. 25 (a) TI photoluminescence spectra of KY_3F_{10} single crystal at 295 (red symbols) and 6.6 K (yellow symbols). The PL emission spectra excited by 13 eV (a) and 26 eV (b) excited by VUV photons. TI excitation spectra for the 4.5 eV emission recorded at 6.6 K for the 4.5 eV emission recorded at 6.6 K (c) and for the 4.77 eV emission recorded at 295 K (d).

The photon energy range 16- 34 eV depicted in Fig. 25 (c, d), due to the limited access (COVID pandemic) to MAX IV Lab only time-integrated studies have been performed so far. Thus, advantages from time-resolved spectroscopy cannot be used in the analysis of KY_3F_{10} data like for BaY_2F_8.

According to the literature overview and recent results on KYF_4 published in Ref. [36], the K 3p cross-luminescence onset is E_{gc} = 20.8 eV. Near 21 eV one can see the decrease excitation intensity at 295 and 6.6 K, thus no spectral features corresponding to the cross-luminescence excitation onset E_{gc} due to ionization of K 3p core level cannot be identified for KY_3F_{10} using time-integrated excitation spectra. The broad excitation bands are tentatively assigned to the overlap of various interbond transitions with those due to the formation of K 3p cation excitons as observed in all wide gap crystals. According to the AFLOW electronic band structure calculations (see Fig. 6) the spin-orbit split Y^{3+} 4p states form bands 17.3 – 18.8 eV and 19.7 -

21.1 eV below the top of the valence band. The analysis of excitation spectra near intrinsic absorption edge (see above) provided that $E_g \sim 11.4$ eV. Therefore, combining electronic band structure data with the experimental energy gap suggests that the Y^{3+} 4p states should be observed in the energy range 28.7 – 32.5 eV, which is in good agreement with the excitation spectra shown in Fig. 25. (c, d). It is also obvious that Y states do not contribute to the cross-luminescence process as these are located energetically deeper than the K 3p level.

According to theoretical calculations, the width of the valence band in KY_3F_{10} is ~3.1 eV, and the K 3p level is located at 9.3 eV below the top of the valence band. Thus, the expected low energy edge of cross-luminescence is near 6 eV. In the comparison with the cathodoluminescence spectra shown in Fig.14, there is a decrease in cross-luminescence near 6.0 eV. Below this energy, the other stronger emission spectra overlap with the cross-luminescence and mask its low energy edge. The decay curve (Fig. 24) recorded through the interference filter IF256 (the maximum transmission at 4.82 eV) has sub-nanosecond decay components typical for cross-luminescence. It is no contradiction with the analysis presented here because the transmission of the interference filter extends to the VUV region below 6 eV. The analogous decrease is observed for KYF_4 under soft-ray excitation (Fig. 7), where the intensity of the fast emission component is decreasing towards the UV region. Emissions shown in Fig. 25 (a, b) in the UV and visible range cannot be uniquely identified based on this research. The tentative assignment of the emission bands near 5 eV allows us to relate these to defect centers formed during the crystal growth. The radiative decay of STE is tentatively assigned to the emission peaked at 3.6 eV (Fig. 25 (a, b)) based on the analogy of electronic properties with KYF_4 single crystal, where STE emits at 3.8 eV [35].

SUMMARY

The present study was devoted to the investigation and identification of various kinds of intrinsic emissions in BaY_2F_8 and KY_3F_{10} single crystals. Both compounds belong to the materials with cross-luminescence, which is due to the recombination of electrons from the valence F 2p states with Ba 5p or K 3p core holes, respectively. The luminescence properties of BaY_2F_8 have been studied under VUV excitation earlier, however the KY_3F_{10} crystal was investigated for the first time. The extensive spectroscopic studies were performed using cathodoluminescence and time resolved luminescence spectroscopy under synchrotron radiation at various temperatures. The obtained experimental results were used to identify electronic band structure parameters such as the exciton formation energy E_{exc}, the energy gap value E_g and the ionization energy of cation levels (cation energy gap E_{gc}). These values were compared with those available from the band structure calculations in the public databases of materials properties like the AFLOW and Materials Project database.

It was found that in BaY_2F_8 cross-luminescence covers the energy range from 7.6 to 5.0 eV, and its excitation onset is at 19.3 eV. The energy gap value estimated $E_g \sim 11.4$ eV was found to be smaller than the 12.4 eV value determined earlier. Thus, the Ba 5p are separated from the top of the valence band by 7.9 eV, which agrees well with the experimentally determined high energy edge of cross-luminescence at 7.6 eV. Low temperature luminescence bands in the UV – visible range are shown to be non-elementary, consisting of the STE emission peaked at 4.96 eV (E_{exc}=10.35 eV) with microsecond decay time and some defect or impurity emission peaking at 3.8 eV. Decay kinetics analysis performed for ultrafast UV emissions show that they contain three exponential components with τ_1=110 ps, τ_2=430 ps and τ_3=5 ns, which is typical for cross-luminescence.

In KY_3F_{10} single crystal, cross-luminescence was revealed in the energy range from 9.1 to 6.0 eV in cathodoluminescence experiment. Due to a limited access to the MAX IV Lab in a lasting pandemic period, no time resolved emission and excitation spectra were studied, prohibiting revealing the ionization threshold of the K 3p cation states with the same confidence as for BaY_2F_8. The excitation peak for 4.5 eV emission observed at 9.9 eV near the intrinsic absorption edge is assigned to the creation of excitons and the energy gap value is estimated to

E_g ~ 11.4 eV. The analysis of time integrated excitation spectra for UV emission (4.5 and 4.77 eV at 6 and 295 K, respectively) revealed several features in the energy range of 28.7 – 32.5 eV, which according to the calculated electronic band structure data are due to the contribution of the Y 4p states. Since the Y 4p states are energetically below the K 3p levels, these cannot participate neither in the cross-luminescence process nor in other excitation processes related to the valence band. The UV emissions near 5.0 eV are tentatively assigned to defect and impurity centers, while a broad emission band with maximum at 3.6 eV is attributed to STE. In the decay kinetics of the UV luminescence in KY_3F_{10}, three exponential components with τ_1=45 ps, τ_2=625 ps and τ_3=3.27 ns were identified.

This research carried out in the framework of the present Master Thesis undoubtedly shows how important is to combine contemporary time-resolved spectroscopic investigations at modern light sources and the results of advanced electronics structure calculations in order to understand luminescence properties of wide gap scintillators. Such analysis greatly promotes a progress in scintillator science and technology of optical materials urgently needed in many applications.

KOKKUVÕTE

Käesolev töö on pühendatud erinevate omakiirguste uurimisele ja identifitseerimisele BaY_2F_8 ja KY_3F_{10} monokristallides. Mõlemad uuritavad ühendid kuuluvad materjalide hulka, milles on leitud kross-luminestsents, mis tekib F 2p valentselektronide rekombinatsioonil, vastavalt kas Ba 5p või K 3p katiooni aukseisunditega. BaY_2F_8 kristalle on varasemalt uuritud kasutades fotoergastust VUV spektraalpiirkonnas, aga KY_3F_{10} kristalli puhul see on esmakordne uuring. Töö käigus viidi läbi mahukad spektraaluuringud kasutades katoodluminestsentsi ja ajalise lahutusega luminestsentsspektroskoopiat ergastamisel sünkrotronkiirgusega erinevatel temperatuuridel. Saadud eksperimentaalsetest andmetest määrati sellised ainete elektronstruktuuri parameetrid nagu eksitonide tekitamise energia E_{exc}, keelutsooni laius E_g ja katioonseisundite ionisatsiooni energia (katiooni keelutsooni laius E_{gc}). Saadud väärtusi võrreldi teoreetiliste arvutuste tulemustega, mis on kättesaadavad avalikes andmebaasides nagu AFLOW ja Materials Project.

BaY_2F_8 puhul leiti, et kross-luminestsents katab energia piirkonna 7.6 – 5.0 eV ning selle ergastuslävi asub 19.3 eV. Keelutsooni laiuseks hinnati $E_g \sim 11.4$ eV, mis on väiksem varasemalt saadud tulemusest 12.4 eV. Seega, Ba 5p seisundid asuvad valentsitsooni laest 7.9 eV kaugusel, mis on heas kooskõlas eksperimentaalselt määratud kross-luminestsentsi spektri servaga 7.6 eV juures. Madalatemperatuursed kiirgusribad UV ja nähtavas spektraalpiirkonnas on mitte-elementaarsed ja koosnevad iselõksustunud eksitoni kiirgusest maksimumiga 4.96 eV (E_{exc}=10.35 eV), mille eluiga on mikrosekundites, ning defekti-lisandi kiirgusest 3.8 eV. Ülikiire UV kiirguse kustumiskineetika analüüs näitas, et seda saab lähendada kolme eksponentfunktsiooniga, mis annavad eluigadeks τ_1=110 ps, τ_2=430 ps ja τ_3=5 ns. Need on tüüpilised väärtused kross-luminestsentsile.

KY_3F_{10} kristalli jaoks leiti, et kross-luminestsents katab energia piirkonna 9.1 – 6.0 eV. Kahjuks pandeemia ei võimaldunud MAX IV laboris läbi viia aeglahutusega kiirgus- ja ergastusspektrite uuringuid, mistõttu ei olnud võimalik määrata katioonseisundite ionisatsiooni energia väärtust analoogselt BaY_2F_8 kristalliga. Fundamentaalneeldumise serval leitud ergastusriba 9.9 eV, 4.5 eV kiirguse jaoks, on seotud eksitonide tekkega ning keelutsooni väärtuseks hinnati $E_g \sim 11.4$ eV. Ajaliselt integreeritud UV kiirguse ergastusspektritest leiti, et struktuurid 28.7 – 32.5 eV piirkonnas on seotud Y 4p ergastustega vastavalt teoreetilistele tsoonistruktuuri arvutustele. Seega Y 4p seisundid asuvad sügavamal kui K 3p seisundid ja

seepärast ei võta osa nii kross-luminestsentsiga seotud kui ka teisestest valentsergastustega seotud protsessidest. UV kiirgused 5.0 eV ümbruses on esialgselt tõlgendatud defekti-lisandi tsentrite kiirgusega ning laiaribalise iselõksustunud eksitoni kiirguse asukohaks spektris on riba 3.6 eV juures. KY_3F_{10} UV kiirguse kustumiskineetikas leiti kolm eksponentsiaalset komponenti eluigadega τ_1=45 ps, τ_2=625 ps ja τ_3=3.27 ns.

Selle magistritöö raames tehtud uuringud näitavad ilma kahtluseta kui oluline on kasutada kaasaaegseid ajalise lahutusega spektroskoopilisi uuringuid koos modernsete valgusallikatega ning kaugele arendatud tsoonistruktuuri teoreetiliste arvutuste tulemusi, et aru saada laia keelutsooniga stsintillaatorite luminestsentsomadustest. Sellised materjalide omaduste analüüsid aiatavad kaasa progressile stsintillaatorite uuringutes ning optiliste materjalide tehnoloogias, mida vajatakse paljudes rakendustes.

REFERENCES

[1] R. Ronda, Cornelis, ed., "*Luminescence: from theory to applications"*. John Wiley & Sons, 1-3 (2007)

[2] R. T. Williams, and K. S. Song., "The self-trapped exciton". *Journal of Physics and Chemistry of Solids* 51, no. 7 680 (1990).

[3] V. N. Makhov, M. A. Terekhin, M. Kirm, S. L. Molodtsov, and D. V. Vyalikh. "A comparative study of photoemission and cross luminescence from BaF_2." *Nuclear Instruments and Methods in Physics Research Section A: Accelerators, Spectrometers, Detectors and Associated Equipment* 537, no. 1-2: 113-116 (2005).

[4] V. Eijk, C. W. E. "Cross-luminescence." *Journal of luminescence* 60: 936-941 (1994).

[5] J. Saaring, E. Feldbach, V. Nagirnyi, S. Omelkov, A. Vanetsev, and M. Kirm. "Ultrafast Radiative Relaxation Processes in Multication Cross-Luminescence Materials." *IEEE Transactions on Nuclear Science* (2020).

[6] Li, Shunran, Jiajun Luo, Jing Liu, and Jiang Tang. "Self-trapped excitons in all-inorganic halide perovskites: fundamentals, status, and potential applications." *The journal of physical chemistry letters* 10, no. 8 (2019): 1999-2007.

[7] N. N. M. Y. Chan, A. Idris, Z. H. Z. Abidin, H. A. Tajuddin, and Z. Abdullah. "White light employing luminescent engineered large (mega) Stokes shift molecules: a review." *RSC Advances* 11, no. 22 (2021): 13409-13445.

[8] M. Kirm, A. Lushchik, Ch. Lushchik, A.I. Nepomnyashikh, F. Savikhin, Dependence of the efficiency of various emissions on excitation density in BaF_2 crystals, Radiation Measurements 33, 515-519 (2001).

[9] M. Kirm, S. Vielhauer, G. Zimmerer, A. Lushchik, Ch. Lushchik, *Cation and Anion Electronic Excitations in MgO and BaF_2 Crystals under Excitation by Photons up to 75 eV* Surface Review and Letters **9**, 1363-1368 (2002).

[10] N.Yu. Kirikova, V.E. Klimenko, V.A. Kozlov, V.N. Makhov, N.M. Khaidukov, T.V. Uvarova, Cross-luminescence of several complex fluorides excited by synchrotron radiation, Nucl. Instr. and Meth. in Phys. Res. A 359, 351-353 (1995). https://doi.org/10.1016/0168-9002(94)01383-7.

[11] J. Jansons, Z. Rachko, J. Valbis, J. Andriessen, P. Dorenbos, C.W.E. van Eijk, N.M. Khaidukov, Cross-luminescence of complex halide crystals, J. Phys.: Condens. Matter 5, 1589-1596 (1993).

[12] Yu M. Aleksandrov, I. L. Kuusmann, V. N. Makhov, S. B. Mirov, T. V. Uvarova, and M. N. Yakimenko. "Intrinsic and impurity cross-luminescence in three-component barium-containing compounds." Nuclear Instruments and Methods in Physics Research Section A: Accelerators, Spectrometers, Detectors and Associated Equipment 308, no. 1-2: 208-210 (1991).

[13] M. Kirm, A. Lushchik, Ch. Lushchik, V. Makhov, E. Negodin, S. Vielhauer, G. Zimmerer, *VUV luminescence of BaF_2, BaF_2:Nd and BaY_2F_8 crystals under inner-shell excitation,* Nucl. Instr. Meth. A **486,** 422-425 (2002).

[14] I.A. Kamenskikh, M.A. MacDonald, V.N. Makhov, V.V. Mikhailin, I.H. Munro, M.A. Terekhin, Fast crystalline scintillators for high counting rate X-ray detectors, Nucl. Instrum. Methods Phys. Res. Sect. A 348, 542-545 (1994).

[15] P. Schotanus, P. Domenbos, S.W.E . Van Eijk and H J. Lamfers, Nucl. Instr. and Meth. A281, 162 (1989).

[16] O. Isayev, C. Oses, C. Toher, E. Gossett, S. Curtarolo, and A. Tropsha. "Universal fragment descriptors for predicting properties of inorganic crystals." *Nature communications* 8, no. 1: 1-12 (2017).

[17] Bassani, Franco. Encyclopedia of condensed matter physics. Elsevier acad. press, 395-402 (2005). https://doi.org/10.1016/B0-12-369401-9/00445-9.

[18] M. Kirm, S. Vielhauer, G. Zimmerer, A. Lushchik, Ch. Lushchik, *Cation and Anion Electronic Excitations in MgO and BaF_2 Crystals under Excitation by Photons up to 75 eV* Surface Review and Letters **9,** 1363-1368 (2002).

[19] J. Andriesen, P. Dorenbos, C.W.E. van Eijk, Molecular Physics 74(3), 535 (1991).

[20] "Materials project database", https://materialsproject.org/materials/mp-1029/, Doi: 10.17188/1186880.

[21] A. B. Adriano, G. F. da C. Bispo, Z. S. Macedo, S. L. Baldochi, E. G. Yukihara, and M. E.G. Valerio. "VUV excited luminescence and thermoluminescence investigation on Er^{3+}-or Pr^{3+}-doped BaY_2F_8 single crystals." Optical Materials 90, 238-243: (2019).

[22] "Material project database", https://materialsproject.org/materials/mp-768240/, Doi: 10.17188/1298305.

[23] "Automatic Flow for material discovery", http://aflow.org/material/?id=aflow:9fc8ca9f354c8449, (ICSD#183922).

[24] M. Diaf, E. Boulma, and Z. Chouahda. "Synthesis and optical properties of KY_3F_{10} laser material doped with rare earth ions (erbium: Er^{3+})." *Photonics, Devices, and Systems II*. Vol. 5036. International Society for Optics and Photonics, (2003).

[25] Norman P. Barnes, "Solid-state lasers from an efficiency perspective." *IEEE Journal of Selected Topics in Quantum Electronics* 13, no. 3: 435-447 (2007).

[26] "Material Project database", https://materialsproject.org/materials/mp-2943/, Doi: 10.17188/1203830.

[27] V.N. Makhov, N.M. Khaidukov, Cross-luminescence peculiarities of complex KF-based fluorides, Nucl. Instr. and Meth. in Phys. Res. A 308 (1991) 205-207, doi:10.1016/0168-9002(91)90627-3.

[28] N.Yu. Kirikova, N.M. Khaidukov, V.E. Klimenko, V.A. Kozlov, V.N. Makhov, T.V. Uvarova, Cross-luminescence of multi-component fluoride crystals excited by synchrotron radiation, Record of the Int. Workshop "PHYSCI-94" Physical Processes in Fast Scintillators, St. Petersburg, September 30 - October 3, 1994, p.172-181.

[29] "Material Project database", https://materialsproject.org/materials/mp-2943/, Doi: 10.17188/1203830.

[30] "Automatic Flow for material database", http://aflow.org/material/?id=aflow:b88a0eec1aa50936, (ICSD#155137).

[31] E. Feldbach, E. Tõldsepp, M. Kirm, A. Lushchik, K. Mizohata, and J. Räisänen. "Radiation resistance diagnostics of wide-gap optical materials." *Optical Materials* 55: 164-167 (2016).

[32] V. Pankratov, R. Pärna, M. Kirm, V. Nagirnyi, E. Nõmmiste, S. Omelkov, S. Vielhauer, K. Chernenko, L. reisberg, P. Turunen, A. Kivimäki, E. Kukk, M. Valden, M. Huttula "Progress in development of a new luminescence setup at the FinEstBeAMS beamline of the MAX IV laboratory." *Radiation Measurements* 121: 91-98(2019).

[33] A.A. Kaminskii and T.V. Uvarova, Izvestiya Academii Nauk SSSR, ser. Neorganicheskie Materialy 24 (1980) 2080.

[34] N.M. Khaidukov, T.G. Filatova, M.B. Ikrami, P.P. Fedorov, Morphotropy in lanthanide fluoride series. *INORGANIC MATERIALS*, *29*(7), (1993) 1152-1156.

[35] J. Becker, M. Kirm, V.N. Kolobanov, V.N. Makhov, V.V. Mikhailin, A.N. Vasil'ev, G. Zimmerer, Coexistence of triplet and singlet emission in alkaline earth fluoride crystals, The Electrochemical Society Proceedings Series: Excitonic Processes in Condensed Matter PV 98-25 (1998) 415-419, Eds. R.T. Williams and W.M. Yen.

[36] Vladimir N. Makhov, Alexander S. Vanetsev, Nikolai M. Khaidukov, Andrei N. Belsky, Min Yin, XianTao Wei, and Aleksei Kotlov, Crossluminescence of Nanosized KYF_4, IEEE TRANSACTIONS ON NUCLEAR SCIENCE, 59, 2102-2105 (2012).

Appendix

I. Licence

Non-exclusive licence to reproduce thesis and make thesis public

I, **Shania Roy,**

1. herewith grant the University of Tartu a free permit (non-exclusive licence) to reproduce, for the purpose of preservation, including for adding to the DSpace digital archives until the expiry of the term of copyright,

   Investigation of luminescence properties of wide gap BaY_2F_8 and KY_3F_{10} single crystals by means of luminescence spectroscopy., supervised by **Prof. Marco Kirm**.

2. I grant the University of Tartu a permit to make the work specified in p. 1 available to the public via the web environment of the University of Tartu, including via the DSpace digital archives, under the Creative Commons licence CC BY NC ND 3.0, which allows, by giving appropriate credit to the author, to reproduce, distribute the work and communicate it to the public, and prohibits the creation of derivative works and any commercial use of the work until the expiry of the term of copyright.
3. I am aware of the fact that the author retains the rights specified in p. 1 and 2.
4. I certify that granting the non-exclusive licence does not infringe other persons' intellectual property rights or rights arising from the personal data protection legislation.

Shania Roy

04/06/2021